Design and Evaluation of a Plant-controlled Atmometer for Measuring Crop Evapotranspiration

by

Mujibur Rahman

A Thesis submitted to the Faculty of Graduate Studies of

The University of Manitoba

in partial fulfillment of the requirements of the degree of

MASTER OF SCIENCE

Department of Biosystems Engineering

University of Manitoba

Winnipeg

Abstract

Efficient irrigation is one of the critical factors when it comes to economically viable and sustainable crop growth to increase yields substantially. The primary objective of this study was to design and evaluate a plant-controlled atmometer for measuring crop evapotranspiration. The specific objectives of this study were to 1) design and evaluate a plant-controlled atmometer which will consider both weather variables and soil moisture status, 2) calibrate the capacitive soil moisture sensors in different types of soil and compare the actual volumetric water content (VWC) to the volumetric water content obtained by the gravimetric method in three different soil types. The plant-controlled atmometer porous ceramic plate was calibrated by measuring the evaporation rate under a different negative pressure head. Two types of capacitive soil moisture sensors (SKU: SEN0193 and SEN0308) were calibrated in the lab using three soil textures (i.e., sand, clay, and loam) to understand the root zone moisture status better. As a plant-controlled atmometer will consider weather and soil moisture status, it is necessary to measure the soil moisture using a sensor that can be incorporated with the programming of the systems. The performance of the sensors when placed in the field was then compared. The calibration results demonstrated a strong association between the sensor voltage reading and the computed VWC obtained from the gravimetric method. The sensor voltage value decreased as the soil water content increased from dry to saturated. In SKU: SEN0193 sensors, the coefficient of determination (R^2) in linear regression and root means square error (RMSE) were 0.96 and 0.0138, 0.93 and 0.0237, and 0.96 and 0.0143 for sand, clay, and loam, respectively. In the case of SKU: SEN0308, the values for the three soil textures were 0.96 and 0.0078, 0.93 and 0.0239, and 0.92 and 0.0169, respectively. In the case of 2nd-order polynomial regression, the R^2 and RMSE of sand, clay, and loam were 0.98 and 0.0101, 0.99 and 0.0102, 0.96 and 0.0143, respectively, for SKU: SEN0193 sensors, while for SKU: SEN0308 sensors, the values of metrics were 0.97 and 0.0068, 0.95 and 0.0197, 0.95 and 0.0133, for the three soil textures respectively. It was found that the evaporation rate is higher with a lower negative pressure head. The R^2 of 2nd-order polynomial regression between evaporation and negative pressure head was 0.95, 0.83, and 0.97, respectively. An Arduino programming code was written considering this relationship to run the plant-controlled atmometer to control the ET rate and the pressure changes during that period. It was found that the pressure changes with the increasing and decreasing trend of ET. When the negative pressure imposed on the water supply side of the porous ceramic plate changed from 0 to 0.8 mH_2O, the evaporation rate changed from 7.0 mm/day to 1.6 mm/day, respectively. The evaporation rate from the plant-controlled atmometer was controlled by imposing a negative pressure simulating a lower soil water content. The field testing of the plant-controlled atmometer simulated lower evaporation rates when the soil water content decreased.

Acknowledgement

First of all, I would like to praise and thank Allah for bestowing innumerable gifts and opportunities to complete my thesis.

The success of this research is highly reliant on the advice and support of many others. This is my chance to express my gratitude to Dr. R. Sri Ranjan, my thesis advisor, for his essential suggestions, helpful criticism, and constant support during this project. In fact, I could not have asked for a greater partner because he is always willing to go above and beyond. I would like to thank my review committee members, Dr. Chyngyz Erkinbaev and Dr. Marcos Cordeiro, for their invaluable contributions to my research.

I am very thankful to the Biosystems Engineering staff at the University of Manitoba, especially Matthew McDonald, for their help completing this thesis.

The friendship and encouragement from many of my friends and lab mates have been invaluable to my work. I am thankful to Sampson, Rahul, Dasinja, Thushyanthy, Ishmeet, Harmeen, Prabakaran, Emeka, and Ifeoluwa. For motivating me throughout this journey, I would like to specifically thank my friends, Md. Shahadat Hossain, MD. Soumik Farhan and Ahmed Salman.

I would also like to express my gratitude to the Bell/MTS funds for the development of IoT in Agriculture, the Natural Sciences and Engineering Research Council (NSERC), and the Graduate Enhancement of Tri-Agency Stipends (GETS) for their financial assistance in this research.

Last but not least, I will forever be indebted to my parents for their unwavering support and to my gorgeous sister Farhana and her husband, Mir Rabbi, for their kindness and generosity.

Dedication

To my lovely family

Table of Contents

List of Tables

List of Figures

List of Symbols

ET_p	Potential Evapotranspiration
ET_a	Actual Evapotranspiration
IoT	Internet of Things
ET	Evapotranspiration
PM	Penman-Monteith
MD	Molecular Dynamics
ET_o	Reference Evapotranspiration
CWR	Crop Water Requirement
IWR	Irrigation Water Requirement
VWC	Volumetric Water Content
GWC	Gravimetric Water Content
MCUs	Microcontrollers
IDE	Integrated Development Environment
API	Application Programming Interface
GSM	Global Service Message
RMSE	Root Mean Square Error
MAD	Mean Absolute Deviation

Chapter 1 Introduction

1.1 Overview

Water is essential for the survival and optimum growth of plants. As a result of climate change, available water resources for agricultural purposes are diminishing in many parts of the world, with more of a focus placed on dry and semi-arid regions. It is necessary to accurately assess the amount of water used by crops to enhance water management and achieve greater water use efficiency in agricultural production. The Actual Evapotranspiration (ET_a) of the crop has to be precisely determined for improved irrigation planning and to reduce the detrimental consequences of over- and under-watering on crop yield and the environment. Estimating the amount of water used by crops can be accomplished directly or indirectly. The lysimeter is a device used to determine the ET_a accurately (Irmak et al. 2006; Irmak, Payero, et al. 2005). In the absence of the aforementioned sophisticated techniques, another approach for indirectly estimating ET_a is available: the check-book method (Broner 2004; Broner and Law 1991; Djaman and Irmak 2013). The two-step technique is another approach that can be used to estimate ET_a. This approach calls for a precise calculation of the ET_p and the locally determined crop coefficient. Therefore, crop water usage is approximated by multiplying the ET_p by a crop-specific coefficient. This factor depends on several parameters, one of which is the crop type and stage of growth (Djaman et al. 2016; Djaman and Irmak 2013). In all these methods, soil moisture status was not considered while predicting the $ET_{a,}$ causing an overestimation of irrigation requirements in the field.

Most crops in Manitoba do not require additional irrigation because of the generally higher rainfall, except for a few unique crops, including horticulture crops and potatoes. As the demand for potatoes increases, the need for irrigation increases simultaneously to boost production. Due to the increasing demand for potatoes, which accounts for nearly 3/4 of the irrigation, the overall area that is irrigated has expanded every year (Kulshreshtha and Grant 2003). It is necessary to manage well to minimize the water loss in the field as the demand for irrigation is anticipated to increase further. It is crucial to have a better method for calculating the water required by crops to schedule irrigation and manage water resources appropriately. The reference evapotranspiration is calculated directly using equations based on meteorological data such as temperature, humidity, solar radiation, and wind speed (Chen and Robinson 2009).

Understanding the soil moisture state in the plant root zone makes it possible to forecast the plant's water needs accurately. Many approaches and tools are used for measuring the moisture content of the soil, including traditional and modern methods. The thermo-gravimetric methodology is widely acknowledged as the gold standard for estimating soil moisture (Masinda et al. 2022). The sight and feel method, which includes touching the soil, is also used but is time-consuming and laborious (Asif et al. 2015; Vereecken et al. 2008). On the other hand, modern techniques use a wide range of sensors and other equipment. The techniques can detect changes in the amount of moisture present in the soil even before the crop exhibits signs of stress. Measuring devices such as tensiometers, which measure the resistivity of the soil, are easy to use; however, they can only measure a limited range of force levels despite their user-friendliness (Stirzaker et al. 2017). Another popular sensing method is the capacitive soil moisture sensor, adopted due to its long-lasting shelf life and accuracy in the field (Susha Lekshmi et al. 2014).

Less common devices for estimating ET include atmometers. An atmometer is a scientific device used to determine the rate at which water evaporates from a wet surface into the air. Generally, the evaporation rate from the atmometer is used to predict the ET of the plants using crop coefficients, assuming a well-watered condition. However, the ET of the plants declines with a declining soil water content which is not taken into account by the traditional atmometers.

Moreover, traditional atmometers ignore the soil-limiting phase of crop ET. That means it does not account for the reduction in ET if the soil is dry and plants are not transpiring at the maximum rate (Sri Ranjan 2012). Because of this, the current atmometers are unreliable in predicting accurate ET since they tend to overpredict by more than 30% (Irmak, Payero, et al. 2005). On the other hand, the plant-controlled atmometer can overcome this limitation to provide a more reliable estimation of ET.

1.2 Scope and objectives

The primary objective of this research was to build and evaluate a plant-controlled atmometer for real-time irrigation scheduling. The specific aims were:

i. Calibrate the capacitive soil moisture sensors for different types of soil
ii. Design and evaluate a plant-controlled atmometer that will accurately predict crop water requirements.
iii. Using IoT technology, send the real-time irrigation data to the cloud server to access them in real time.

1.3 Thesis arrangement

This thesis is arranged based on the chapters. Chapter 1 provides an outline of the research activity. Chapter 2 is a literature review on evaporation and evapotranspiration, crop water measurement techniques, and sensor-based soil moisture measurements. This section also includes the literature on the internet of things in agriculture. The third and fourth chapters are made up of two manuscripts, each with an abstract of the study, a general introduction, materials and techniques, findings and discussion, and conclusions. The primary focus of Chapter 3 is to assess the performance of two capacitive soil moisture sensors in various soil types for use in building plant-controlled atmometers. Chapter 4 describes the building and evaluating a plant-controlled atmometer for real-time irrigation scheduling. Chapter 5 highlights this study's key findings and suggestions for further research. All the references for this thesis are listed at the end.

Chapter 2 Literature review

2.1 Background: an overview of the atmometer

Over the past few decades, atmometers have been used for measuring the evaporation rate influenced by different weather conditions (Blanco et al. 2004; Irmak, Payero, et al. 2005). This evaporation rate is then converted to crop evapotranspiration (ET) with an appropriate crop co-efficient (Irmak, Dukes, et al. 2005). The crop ET rate is maximum when the soil is wet and characterized by the weather-limiting phase. However, it is difficult for the plant to draw water from the soil when the soil is dry due to high negative pressure (Sri Ranjan 2012). The rate of plant ET declines by stomatal closure, causing a reduction in water flow from the root zone.

A study by Blanco and Folegatti (2004) found that most equipment-based atmometers like the Piche atmometer, reduced pan, and class A pan atmometer overestimated evaporation when the water surface was free, and there was no resistance used from the supply side. The authors used different atmometers in a greenhouse and class A pan outside to compare the ET rates calculated with the Penman-Monteith equation to assess. However, most scientific literature shows an extensive decrease in the use of pan evaporation during the last few decades (Fu et al. 2009; Giambelluca et al. 1992; Sanchez-Lorenzo et al. 2014). Notably, most of the aforementioned studies did not consider windspeed or soil moisture to estimate the ET rate. Among the mentioned evaporation devices, some of them are easy to use, while some have complex functionality.

Pan evaporation is one of the simplest ways of measuring the evaporation rate at which water evaporates into the air from a pan, dish, or similar open container (Brutsaert 2013). A simple pan evaporation model (Pen Pan) was developed based on a modified version of Penman's potential evapotranspiration equation (Rotstayn et al. 2006). Climate elements, such as temperature, rainfall, solar radiation, and wind, are considered in pan-evaporation measurements. The evaporation depth is also measured in pan and atmometer evaporation measurement with ET using crop coefficients. Nevertheless, ET in a plant is controlled by weather conditions and soil moisture content (Sri Ranjan 2012). Thus, the weather-based atmometer or pan evaporation method does not consider the soil water content. Neglecting the plant response to soil moisture deficit leads to an overestimated application of irrigation water depth.

The Penman-Monteith (PM) method has been traditionally used to estimate the reference evapotranspiration (Djaman et al. 2016; Giambelluca et al. 1992; Magliulo et al. 2003), which requires a large number of weather variables. However, alternative equations have been applied to analyze the local weather conditions and compared with the standardized PM method. In a study that used six ET_o equations to calibrate, evaluate, and validate, it was found that the calibration was the major reason for better results of ET_o equations and for adopting the best models for weather conditions (Djaman et al., 2016). However, when data from a weather station is used in empirical equations to predict ET, which is not crop-specific, it can lead to significant errors in the rate of ET and an overestimated irrigation requirement because the soil water content influence is not considered (Sri Ranjan 2012).

A METRIC (Mapping Evapotranspiration at high Resolution with Internalized Calibration) model (Allen et al. 2007; Kjaersgaard et al. 2011; Reyes-González et al. 2017) has also been used to estimate the ET and compare it with the atmometer readings. The objectives were to analyze the variation in ET measurement in satellite-based remote sensing under field conditions. Clear sky images were collected from Landsat 7 and 8 and used for the study. In addition, the atmometer data were recorded during the daytime and compared with the data collected from the satellites (Reyes-González et al. 2017). Only two bimonthly satellite images were compared to the corresponding atmometer data on those days. However, this may not have accounted for the monthly rainfall that affects evaporation. Therefore, one constraint of the suggested methodology is the representativeness and quality of the soil evaporation estimates utilized to calculate background evaporation. Estimating the soil moisture content requires an accurate depiction of the geographical distribution of precipitation. Using surface measurements to calculate rainfall on a pixel-by-pixel basis might cause significant biases (Kjaersgaard et al. 2011).

In another study, Straatmann et al. (2018) studied the validation and uses of an electric atmometer in a humid region and compared the ET values with data obtained from an electric weather station with sensors. It was found that the atmometers underestimated ET relative to the calculated values. Calibration is required before using the ET from atmometers in irrigation scheduling. Only weather conditions were considered during the process, but soil moisture was not considered.

Considering all the above atmometer functionality, estimation of ET based on the traditional methods will lead to inaccuracy and overestimation of the ET, which will cause over-irrigation of crops (Sri Ranjan 2012). It is required to design an atmometer device that can consider not only the weather conditions but also the real-time soil moisture status of the crop fields to increase accuracy in predicting ET.

2.2 Evaporation

Soil water evaporation is the process of exchanging water between soil and atmosphere where plants' physical functioning is involved, which influences the quantity of water loss from the soil by the plants and microorganisms (Lehmann et al. 2008). Measuring the evaporation rate is a complex process, except for lysimeters which measure evaporation based on the changes in water volume (Evett et al. 1995). There are many direct, and indirect approaches (water balance method) used to calculate evaporation. Many variables influence the rate of soil evaporation to calculate soil evaporation precisely. The two significant factors affecting soil evaporation rate are atmospheric conditions, such as humidity, temperature, ambient air speed, and soil pore area, and soil transport characteristics, including thermal conductivity, hydraulic conductivity, and vapour diffusion. These factors lead to complexity in the dynamic interactions between media properties, transport techniques, and boundary prerequisites and effects in an extensive variation in the evaporation activities (van Brackel 1980; Özgür and Koçak 2015; Prat 2002; Sakai et al. 2011).

The evaporation from soil surfaces involves the transfer of mass and energy, including phase transformation, vapour diffusion, and fluid flow, causing a complicated dynamic displacement that impacts the drying rate, which changes over time. The soil water evaporation can be divided into two phases. The first one comprises a comparatively higher and constant initial evaporation rate, whereas the second involves a lower evaporation rate with a regulated vapour diffusion (van Brackel 1980; Kaviany and Mittal 1987; Salvucci 1997; Schultz 1991). The water depletion rate is almost constant per unit surface throughout the initial stage, closer to the evaporation rate from a free water surface. This regular initial rate is noteworthy due to the substantial shift in the medium's fluid flow and the drying front's continuing withdrawal (van Brackel 1980; Shokri et al. 2009; Yamanaka and Yonetani 1999). The first phase ends suddenly with a critical water content or drying front depth and is followed by the lower rate phases, which are regulated mainly by diffusive mass transfer. Numerous reports address the circumstances and methods for regulating pore drying (van Brackel 1980; Lehmann et al. 2008; Sakai et al. 2011). On the other hand, water evaporation starts when the water molecules break by the force of energy.

Though evaporated as the surface phenomenon, the rates of molecular movement across a liquid-vapour interface depend heavily on integrated fluid dynamics and thermal transfer through bulk fluids. Recent experimental thermocouple measurements have shown the role of heat transfer to evaporation in the temperature region near the interface of evaporating water to its vapour. The analysis results uncovered that the evaporation process was regulated by the heat flow to the interface rather than by the molecular transport through the interface (Kazemi et al. 2017).

Excessive evaporation would contribute rapidly to the drying out of the reservoir and a full system collapse. As the liquid volume in the vessel decreases, the air-water interface's location varies over time. The form of an air-fluid meniscus in a reservoir with a specific water volume was suggested as a simple solution. Instant evaporation levels have been estimated using computer fluid dynamics simulations. In micro-reservoirs, evaporation rates may be improved by reducing the reservoir height or increasing the average diameter. Evaporation is often quickly minimized by raising the reservoir height or decreasing the diameter (Scott Lynn et al. 2009).

In the water-air interface, water evaporation occurs by the complete breakage of hydrogen bonds of a single or a group of water molecules and advances to the region of the gas phase. The thermodynamics of the transformation from condensed to the gaseous state have been studied in molecular dynamics (MD). With improved sampling techniques, MD models have been used to illustrate that evaporation can be treated as a ballistic escape from energetic bulk and interfacial water (Varilly and Chandler 2013).

In another study, it was demonstrated that non-hydrogen bonding, such as O-O or H-H interactions are the reasons for water evaporation from water droplets after the collision of both water molecules in MD trajectories (Mason 2011). It was also found by MD simulation that the interfacial water molecule increases a larger momentum by colliding with a similar molecule at the water-vapour interface. It was further revealed that evaporation could be sharply curbed by avoiding the sequential formation of hydrogen bonds (Nagata et al. 2015).

2.3 Crop evapotranspiration

The notion of potential evapotranspiration (PET) was initially proposed in the late 1940s (Allen et al. 1998). It was defined as the amount of evapotranspiration produced in a particular period by large vegetation of short green crops completely shading the ground, of uniform height, and with enough moisture at all times. The fundamental motivation for inventing the potential evapotranspiration concept was to avoid the effects particular to crops during the evapotranspiration process.

The scientific community favorably embraced PET for a while, and it was used as the key concept in estimating agricultural water demand. However, other constraints became apparent over time. The ET rate was not associated with a particular crop in the PET definition. The most significant cause of PET confusion was that multiple crops might be classified as "short green crops," making it challenging to identify which short crop to select. The term "reference crop evapotranspiration" (ET_o) was coined in the early 1980s when researchers recognized PET's ambiguities and limits (Allen et al. 1998).

The fundamental motivation for inventing ET_o was to make it feasible to estimate the evapotranspiration demand of the environment, neglecting the effects of crops, cultivar differences, crop development, or management strategies.

The terms "actual crop evapotranspiration" (ET_a) and "crop evapotranspiration" (ET_c) refer to the quantity of water that a particular crop evaporates over a certain period under current soil water, and weather conditions. Actual crop evapotranspiration is defined as evapotranspiration from disease-free, well-fertilized crops grown in vast fields under optimal soil water conditions, which reach total production under specified climatic conditions. ET_a can be determined by direct methods such as lysimeters or estimated from climatic data by integrating the effect of crop characteristics into ET_o. The ratio of crop ET to reference ET (ET_a/ET_o), called crop coefficient (K_c), is used to relate them as given in the following relationship shown in equation (1).

$$ET_a = ET_o \ x \ K_c \quad (1)$$

Where, ET_a = Actual crop evapotranspiration (mm/day); ET_o = Reference crop evapotranspiration (mm/day); and K_c = Crop coefficient

2.4 Crop water requirement

The crop water requirement (CWR) is the amount of water needed for a crop to grow optimally without losing yield (Brouwer and Heibloem 1986). The CWR depends on weather conditions (i.e., sunlight, temperature, humidity, windspeed), soil type, crop type, and the crop's growth stage. The maximum crop water is required in hot, dry, windy, and sunny areas. In contrast, minimum water is needed in a cool, humid, and cloudy area with the minimal wind (Brouwer and Heibloem 1986).

The CWR must be supplemented by irrigation water requirements (IWR) when discussing irrigated crops. The IWR refers to the net depth of water (millimetres) that must be applied to a crop to fully satisfy that crop's particular crop water requirement. The IWR is the proportion of the CWR that is not met by the combined effects of precipitation, soil water storage, and groundwater input. The water depth is also included in IWR when a leaching fraction is necessary to guarantee that sufficient salt leaching occurs in the soil profile. In reality, IWR must be translated into gross irrigation demands to account for the irrigation systems' effectiveness (Pereira and Alves 2013; Smith et al. 1998).

2.5 Traditional methods of soil moisture measurement

The most commonly used soil moisture measurement methods are gravimetric soil moisture and volumetric water content (VWC) (Sharma 2018). Gravimetric moisture content measures the amount of water present in a soil sample by weight. At the same time, the VWC is the moisture content present on a volume basis in the soil sample.

2.5.1 Gravimetric soil moisture content

Thermogravimetric analysis requires the removal of soil samples and analysis in the lab, which is exceedingly time-consuming. Moreover, readings are not reproducible. The procedure consists of a cylindrical soil sample collected via a sampling ring of 5 cm height and 80 cm^2 cross-section being weighed before and after oven-drying the sample at 105°C, generally for 48 hours, in the current investigation. The dry basis gravimetric water content is calculated using the following equation:

$$\theta_g = \frac{M_{wet} - M_{dry}}{M_{dry}} \tag{2}$$

Here, θ_g represents the gravimetric moisture content, M_{wet} - mass of the wet sample soil, and M_{dry} - mass of the dry sample soil

2.5.2 Volumetric water content

The volumetric water content (VWC) of soils is essential in agriculture, soil science, soil physics, and geotechnical projects. Various aspects of a porous medium, such as its water retention qualities, volume compressibility, infiltration capacity, and reactivity, are substantially influenced by the value of VWC. Electronic capacitive sensors for assessing volumetric water contents have recently become a well-known technique in various geo-environmental and agricultural applications. Such sensors have the potential to be used for performance assessment and field monitoring of crop fields, gardening, and landfill cover system, among other things. However, there is a possibility that the output of these sensors will not accurately reflect the actual field condition. It is critical to evaluate the functioning of such sensors in the field before deploying them to determine their effectiveness in monitoring various parameters. If there is an abnormality in the readings from the sensors, it must be addressed by following appropriate processes to get representative data.

$$\theta_v = \frac{M_{wet} - M_{dry}}{M_{dry}} \times \frac{\rho_s}{\rho_w} \tag{3}$$

Here, θ_v represents the volumetric water content, M_{wet} - mass of the wet sample soil, M_{dry} - mass of the dry sample soil, ρ_s - Bulk density of sample soil, and ρ_w - density of water

The use of electronic capacitive sensors to determine the volumetric water content is a well-established technique used in a wide variety of geo-environmental and agricultural applications. These sensors may be used to evaluate the landfill cover system's effectiveness and conduct field monitoring. There is a possibility that the output of these sensors will not accurately match the field environment. Before deploying such sensors in the field, it is critical to test their performance to determine their measurement efficiency. If there is an error in the sensor readings, it must be addressed using a proper calibration technique.

2.6 Sensors based soil moisture measurement

In several natural resource management studies, including investigations into agricultural productivity, management of watersheds, monitoring of the environment, precision agriculture, and irrigation scheduling, sensors for measuring soil moisture have been used widely for the last few years. By using soil moisture sensors and getting a real-time moisture status of the field, farmers can make informed decisions about whether to start watering their crops and when to stop doing so if they know the moisture status of the soil. As a result, they can get the most out of the water they utilize while still producing high-quality crops. In addition, irrigation timing is crucial for meeting the water needs of a particular crop, which might be advantageous for irrigators. This is because planned irrigation reduces chemical percolation and nitrogen loss in the soil, both detrimental to environmental quality (Hanson et al. 2000; Leib et al. 2002).

The monitoring and evaluation of soil moisture levels in contemporary agriculture can be carried out with various instruments and methods credited to technological advancements. Some of these soil moisture sensors are tensiometers, resistance blocks, gravimetric methods, and granular matrix sensors that have been extensively used for irrigation scheduling for a number of decades and will continue to be utilized in this capacity to a significant extent. The operation of each of these different irrigation management systems and pieces of equipment requires varying degrees of accuracy and differs in the amount of work necessary, the finishing investment needed, and the level of complexity (Leib et al. 2003; Marazky et al. 2011; Stevens 2007). Over the last few years, several studies have been carried out to assess soil moisture devices both qualitatively and quantitatively in terms of the requirements for setting them up, the maintenance required, the initial cost, the accuracy, and how the data should be interpreted. At the same time, the sensor industry and the rapidly developing computer technology have contributed to developing a wide range of novel advanced sensors (TEROS 12, SMRT-Y) that can be used for irrigation scheduling. These sensors can monitor various environmental factors, including temperature, humidity, and light levels. The newly designed sensors can give real-time monitoring that is both precise and continuous of the soil's moisture content.

When it comes to efficient water management on the farm, specific emphasis should be given to the timing of the irrigation and the amount of water that is put into the system. Using the information on crop evaporation and transpiration and sensor technologies dependent on soil moisture, scientific irrigation scheduling (SIS) is a one-of-a-kind method that accurately calculates when and how much water should be applied to crops. SIS combines these factors uniquely (Leib et al. 2003). If this technology were used in commercial farming operations, it would lead to water management that is both timely and efficient. This would be a significant benefit to the agricultural industry. When deciding how much water to apply for daily irrigation throughout the growing season for strawberries and potatoes that are grown either in open fields or in high tunnels, it is necessary to take into account the amount of available soil moisture, the current weather, the growth stage of the plants, and the temperature of air and soil simultaneously. Since these factors change over time, determining the optimal time to irrigate requires numerous measurements of the soil's moisture content at various depths. This is necessary to make accurate irrigation scheduling. Thus, technology is an essential component of today's contemporary commercial agriculture and plays an integral part in the administration of numerous crop areas of farms. In particular, technologies that monitor the moisture content of the soil have been shown to help corporate producers manage irrigation.

There are many methods for quantifying moisture in the soil. Among them are the following: Finding a system that can recognize both the quantity of frozen water and the amount of water that is not frozen might be a challenging task. A Time-domain reflectometer (TDR) measurement may calculate the amount of water that has not yet frozen. The TDR probe uses the dielectric constant of a third-order polynomial to measure the volumetric water content. This permits the probe to represent the actual water content more precisely. This polynomial is based on the relationship between volumetric water content and wet soil dielectric constant (Adelakun and Sri Ranjan 2013; Bierman 2005; Singh et al. 2019).

2.7 Internet of things in agriculture

The term Internet of Things (IoT) usually refers to situations in which network connectivity and computing power are added to objects, sensors, and other everyday items that are not traditionally thought of as computers. This allows these devices to create, share, and use data with minimal human intervention. Implementations of the Internet of Things use various technical communication models, each of which has different features. Back-End Data-Sharing, Device-to-Device Communications, Device-to-Cloud Communications, and Device-to-Gateway Communications are the primary communication models outlined by the Internet Architecture Board. These models illustrate the versatility of how the Internet of Things devices can link to one another and provide benefits to the user (Kramp et al. 2013; Rose et al. 2015).

Kevin Ashton originated the phrase "internet of things" in 1999, followed by the Massachusetts Institute of Technology (Kramp et al. 2013). At the time, the IoT was entirely reliant on people since almost all Internet-accessible data was acquired or produced by humans. The IoT has the potential to revolutionize everything thoroughly, but it cannot happen without specific prerequisites being met first. (e.g., computer power, sensors, and software) (Ashton 2009).

It was predicted that by 2020, fifty billion devices would be linked to the internet (Vermesan and Friess 2013). The Internet of Things (IoT) has already exhibited various unique uses, including home and workplace monitoring systems, precision agriculture, data and supply chain management, and more. The IoT is a vast repository of data that has already been put to good use in a range of ways throughout the world. There are many ways in which the IoT can be used in everyday life, including the monitoring and management of equipment and appliances in our homes and our security systems. There are several benefits to the Internet of Things (IoT), including improved data management systems, smart city infrastructures, and increased economic development in different sectors. An IoT healthcare system may be built by incorporating smart beds and automated medication dispensers that can upload patient data to notify the care team, such as a hospital or a patient's home (Elanthiraiyan and Babu 2015; Elijah et al. 2018; Evans 2011).

In agriculture, IoT technologies have been utilized primarily for diagnostics, control, and monitoring, by giving information obtained by ground-based and aerial-based smart sensors (i.e., weather stations, soil sensors, remote imaging, etc.). IoT has been beneficial to smart and precision agriculture in several agricultural sectors, including disease and pest detection, weed control, cultivation, irrigation, and water quality monitoring, intelligent crop spraying, evaluating field variables like soil monitoring, climate change monitoring, and monitoring the growth and health condition of plants (Ayaz et al. 2019).

IoT-based technologies have been used in water management and irrigation system enhancement. A study by Kamaruddin et al. (2019) proposed an Internet of Things irrigation management and monitoring strategy that used Arduino technology as an intelligent processor. The results demonstrated that, if implemented, a system that utilizes soil moisture content information to regulate an irrigation process may be very successful. When the soil moisture reaches an appropriate level or begins to rain, the irrigation system stops discharging water for irrigation (both clean water and wastewater). Moreover, the proposed method may be utilized for several functions, including wireless communication between sensors, Android applications, and Wi-Fi processors.

In a separate study, the group investigated the application of IoT-designed technologies to optimize the implementation of an automated and intelligent watering system for a greenhouse. The proposed model uses data collected from digital soil moisture and temperature sensors and information gained from an Open Weather Map that predicts approaching precipitation. In addition to energy and water savings, the technology directly increases agricultural output and productivity (Seethalakshmi et al. 2021).

According to Vani and Rao (2016), monitoring and measuring significant agricultural indicators is critical for agricultural development objectives, especially in real-time. Using Cloud for IoT and an Android smartphone, a system was developed to monitor and measure the moisture content of the soil. This system was then tested in a laboratory. The user could view the real-time data gathered using Cloud technology and the Blynk application. Consequently, a timely reaction to these measured soil moistures might be accomplished everywhere, at any time, and in any place. In a recent study, the same research group proposed a solution to a prevalent issue in the agricultural system: analyzing the change of soil moisture on the yield on a daily basis. This research was conducted to address a long-standing problem that has plagued the agricultural sector. The intelligent technologies that were utilized to establish sensors and collect daily readings of the soil's moisture content include IoT, GSM (Global Service Message) communication technology, and Cloud Computing technology. The system they created used Wi-Fi and GSM-based connections to transfer sensor data to cloud storage and mobile devices. In addition to software, specialized hardware was developed. The Thing Speak Cloud Computing technology was utilized to store sensor information. According to the authors, the final system's implementation was straightforward, and moisture level information may be received remotely (Vani and Rao 2019).

Chapter 3 Calibration and performance evaluation of capacitive soil moisture sensors in different types of soils

3.1 Abstract

Accurate soil moisture measurement is critical for successful irrigation water management in agricultural areas. An appropriate irrigation decision can be made by monitoring the soil water content within the root zone. Several soil moisture sensors are available to automatically and cost-effectively monitor soil moisture. In this research, two types of capacitive soil moisture sensors (SKU: SEN0193 and SEN0308) were calibrated in the laboratory with three different soil types, and their ease of installing them in the field was compared. The calibration results revealed a close relationship between the sensor voltage reading and the actual volumetric water content (VWC) calculated from gravimetric water content. The sensor voltage decreased as the soil became wetter. In SKU: SEN0193 sensors, the coefficient of determination (R^2) in linear and root mean square error (RMSE) was 0.96 and 0.0138, 0.93 and 0.0237, and 0.96 and 0.0143 for sand, clay, and loam respectively. In case of SKU: SEN0308, the values were 0.96 and 0.0078, 0.93 and 0.0239, and 0.92 and 0.0169 for sand, clay, and loam soils, respectively. In case of 2nd order polynomial, the R^2 and RMSE were 0.98 and 0.0101, 0.99 and 0.0102, and 0.96 and 0.0143 in SKU: SEN0193 sensors while the SKU: SEN0308 sensors values were 0.97 and 0.0068, 0.95 and 0.0197, and 0.95 and 0.0133 for the three soil textures respectively. The performance of the sensors was adequate in each of the tested soil types. It was clear that the sensors perform in a diverse range of soils in a manner that is distinct from one another, and that each sensor has a unique variation. It is highly recommended that each sensor be calibrated before installation in the field, depending on the type of soil. This will allow for a better measurement accuracy when installed in the field.

Keywords: Soil Moisture, Capacitive soil moisture sensors, Volumetric Water Content, RMSE

3.2 Introduction

Irrigation water management is essential for maximizing agricultural yield for meeting plant water needs and sustaining nutrient absorption in the root zone. Timely irrigation of the field is crucial. Therefore, precisely estimating the amount of crop water requirement is critical. Since water may occupy up to 40 to 50% of the volume of a particular soil, calibration should be performed in each soil type according to the porosity of the soil to ensure an accurate prediction of water content (Eller and Denoth 1996).

Various methods and instruments are used to measure soil moisture content, which may be split into two categories: classical and modern techniques. The thermo-gravimetric approach is recognized as the standard reference method for determining soil moisture content. However, this procedure is time-consuming, labor-intensive, and requires destructive soil sampling. Another technique for determining soil moisture is the look and feel approach, which mainly depends on the farmer's expertise (Du et al. 2016; Susha Lekshmi et al. 2014; Vereecken et al. 2008). At present different sensors and devices capable of detecting soil moisture changes before the crop enters the stress stage have become widely available. Tensiometers, which are used to determine the matric potential of the soil, have been in use for decades. Even though tensiometers are simple to use, their measuring range is limited (Asif et al. 2015; Li et al. 2003; Stirzaker et al. 2017). Another approach for monitoring soil moisture is neutron scattering, which is very expensive and is limited to research purposes only because of the need for Radiation Safety Certification for operation. Soil resistivity is another technique for detecting soil moisture, which may be done by measuring the resistance between two electrodes placed into the soil. Although simple and inexpensive, it needs careful calibration and installation and is impacted by soil salinity (Sreedeep et al. 2004; Susha Lekshmi et al. 2014).

The emergence of open-source and free software has led to a perfect environment for technological improvements (Okasha et al. 2021; Singh 2005). Technology has been evaluated for agricultural applications for decades to oversee diverse farming operations and make educated decisions based on continuous monitoring of fields using various sensors. Over seventy-five percent of the world's freshwater resources are used for irrigation, making it the most water-intensive of all agricultural operations. Additional pressure on freshwater resources is expected in the following decades because of projected climate change and an expected surge in the global population (Li and Lawrence 2017; Regan et al. 2017; Schulz et al. 2020). Hence, traditional methods of irrigation scheduling need to be updated with precision monitoring methods. Low-cost, advanced scientific devices and cutting-edge technology are available to improve various agricultural operations and reduce over-irrigation (Okasha et al. 2021). Many farmers are likely to adopt new technology if it can be made user-friendly and inexpensive.

The use of capacitive sensors for assessing volumetric water contents has recently become a popular technique in various geo-environmental and agricultural applications (Palaparthy et al. 2013; Surya et al. 2020). Such sensors have the potential to be used for performance assessment and field monitoring of crop fields, gardening, and landfill cover system, due to substantially lower costs and ease of use. Since these types of sensors can measure the water content from different depths at a time, they disturb the soil less than the other types of sensors (Adla et al. 2020; Campora et al. 2019; Matula et al. 2016; Srbinovska et al. 2015). However, there is a possibility that the output of these sensors will not accurately reflect the actual field condition. It is critical to evaluate the functioning of such sensors in the field before deploying them to determine their effectiveness. For irrigation scheduling purposes, soil moisture content must be accurately and quickly assessed.

The present study was initiated to find an accurate and efficient soil moisture measurement relationship for capacitive soil moisture sensors. The key objectives of this experiment were to (i) calibrate the capacitive soil moisture sensor for different types of soil; (ii) compare the actual volumetric water content of the soil with the measured volumetric water content of the soils, and (iii) determine the predictive equation for measuring soil moisture content using the sensors for different types of soils.

3.3 Materials and methods

The experiments for this study were carried out at the Soil and Water Engineering Laboratory of the Department of Biosystems Engineering at the University of Manitoba.

3.3.1 Capacitive soil moisture sensor

Capacitance is the quantity of energy stored in a capacitor and is described by equation (4) (Fares and Polyakov 2006; Halliday et al. 1993; Ida 2015).

$$q = CV$$

Or

$$C = \varepsilon_0 \frac{A}{d} \tag{4}$$

In which q = charge, C = Capacitance, V = Voltage, ε_o = Absolute permittivity of the dielectric material used, A = Surface area of the metal, and d = gap between the metal surfaces.

A capacitor is an electrical device that is composed of three parts, i.e., an electrolytic (positive) plate, an electrolytic (negative) plate, and a dielectric (the gap between). Various capacitors are regularly used because of their varying physical forms and construction. In most capacitors, a dielectric substance separates two electrical conductors, usually in the form of metallic plates or surfaces. Capacitive moisture sensors measure capacitance changes as a result of dielectric changes in the electromagnetic field surrounding the electrodes. Capacitive measuring is essentially the measurement of the dielectric created by the soil, with water being the most significant component affecting the dielectric properties. Capacitive soil moisture measurement has several advantages over resistive soil moisture measurement, including the fact that it not only prevents corrosion of the probe but also provides a more accurate reading of the soil moisture content when compared to using a resistive soil moisture sensor which is more influenced by pore water salinity as well. Consequently, there will be no corrosion of the sensor itself since it is not exposed to the soil via its contacts (Eren 2014; Ling et al. 2016). It changes depending on what is around or between the plates. For example, if the amount of water changes in the soil around a capacitor, this will change the capacitance and the sensor oscillator step, which means that the output voltage will also change. Based on the reading, we can use this feature to calculate how much water surrounds the sensor. As sensors consume little power, it is possible to power them with photovoltaic cells or a microcontroller's feed channel. Despite their high-temperature sensitivity and limited detection range, capacitive soil moisture sensors are widely recognized by researchers due to their dependability (Da Costa et al. 2017; Das et al. 2014; Kojima et al. 2016).

3.3.2 Gravimetric soil moisture content

The typical calibration approach, thermogravimetric analysis, necessitates the removal of soil samples and is exceedingly time-consuming. A cylindrical soil sample (collected via a soil sampling ring of 5 cm height and 80 cm^2 cross-sectional area) is weighed before and after oven-drying at 105°C, for 48 hours, in the current investigation. The measured gravimetric water content, θ_g, is calculated as follows:

$$\theta_g = \frac{M_{wet} - M_{dry}}{M_{dry}} \quad (5)$$

Here, θ_g represents the gravimetric moisture content, M_{wet} - mass of the wet sample soil, and M_{dry} - mass of the dry sample soil

3.3.3 Volumetric Water content

The volumetric water content (VWC) of soils is essential in agriculture, soil science, soil physics, and geotechnical projects. Various properties of the soil, such as its water retention, volume compressibility, infiltration capacity, and reactivity, are influenced by the value of VWC. The use of capacitive sensors for assessing volumetric water contents have recently become a popular technique in various geo-environmental and agricultural applications. However, there is a possibility that the output of these sensors will not accurately reflect the actual field condition. It is critical to evaluate such sensors in the field before deploying them to determine their effectiveness in monitoring. VWC is estimated using gravimetric water content and other soil properties, as indicated by equation (6).

$$\theta_v = \frac{M_{wet} - M_{dry}}{M_{dry}} \times \frac{\rho_b}{\rho_w} \tag{6}$$

Here, θ_v represents the volumetric water content, M_{wet} - mass of the wet sample soil, M_{dry} - mass of the dry sample soil, ρ_b - Bulk density of sample soil, and ρ_w - density of water

3.3.4 Sensors

In this experiment, two types of DFRobot Capacitive soil moisture sensors (SKU: SEN0193 and SKU: SEN0308) were used. The SKU: SEN0308 is the newer and more advanced version by DFRobot, which is made waterproof by the manufactured from top to bottom. Instead of using resistive sensors, which are affected be soil salinity, this sensor uses capacitive sensing to monitor the moisture content of the soil, which is preferrable. This sensor is constructed of corrosion-resistant materials, which ensures that it will have a long service life. Putting it into the soil surrounding plants can provide real-time soil moisture data within the rootzone. This sensor is equipped with an onboard voltage regulator, which allows it to operate across a voltage range of 3.3 to 5.5 volts. It is ideal for use with low-voltage microcontrollers (MCUs), both at 3.3V and 5V. The sensor's output voltage ranges from 0 to 3.0 VDC, and its operational current is 5mA. At 15g in weight, it is a lightweight sensor.

Apart from the sensor, an Arduino UNO board, a breadboard, a digital scale, 400 mL containers, and connecting wires were used in this experiment at setup. To properly calibrate the soil moisture sensors, two of the most important parameters, i.e., the volume and weight of wet and dry soil, need to be measured. A digital scale and container were used to precisely measure the amount of water in the soil to compare the readings obtained by the capacitive soil moisture sensor. Fig. 3.1 depicts the schematic diagram of the Arduino UNO and Capacitive sensor connection.

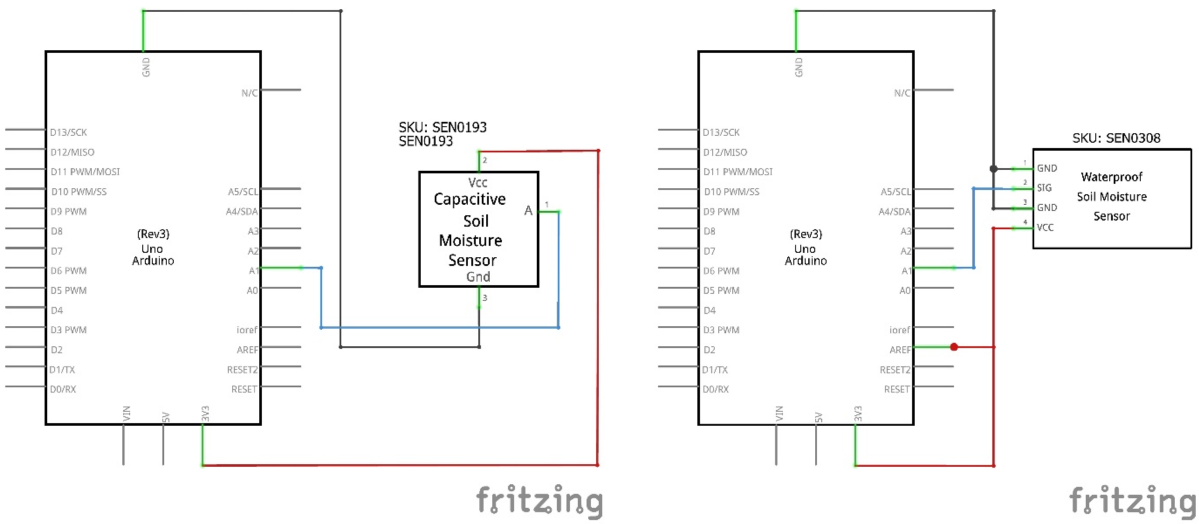

Fig. 3.1 Schematic diagram of the wiring of the SKU: SEN0193 and SKU: SEN0308 sensor with analog reference for the measurement of voltage reading from the capacitive sensor

3.3.5 Calibration procedure of the capacitive soil moisture sensors

At the start of the calibration procedure, the capacitive soil moisture sensor's voltage measurement was taken in the air. The weight of a 400-ml soil sample jar was then measured. After that, dry soil was added to the container until it reached a volume of 300 ml - 350 ml. The mass of the dry soil was determined. The soil was moistened with 10 ml of water and well mixed to ensure even water distribution before refilling the container to 300 ml – 350 ml. Subsequently, the weight of the wet soil in the container was determined and recorded to determine the mass of the wet soil. This procedure was continued until the soil reached saturation. While performing the processes, the voltage measurement of the soil sample was acquired in every step and recorded for calibration purposes. Once the watering procedure was completed, the soil was oven dried for 48 hours, and measured the dry weight of the sample soil.

The calibration procedure of the capacitive soil moisture sensors was performed in different steps. Initially, all three types of soil samples collected from the field were naturally dried for several days before using them in the experiment. The bulk density of the sample soils was calculated during the process. The density of the water was 997 kg/m^3, the container mass was 149 gm, and the soil volume was 300 ml. The bulk density of the sandy soil sample used in the SKU: SEN0193 sensor was measured at 1.680 $g/cm^{3,}$ while the bulk density of the sample used in the calibration of the SKU: SEN0308 was 1.71 $g/cm^{3,}$ and the soil volume was 350 ml, and the container mass was 149 gm.

Similarly, the clay soil sample was collected, and the container weighed 149 gm, while the soil volume was 300 ml and 350 ml for SEN0193 and SKU: SEN0308 sensors, respectively. The bulk density of the clay soil sample was calculated at 1.11 g/cm^3 and 1.194 $g/cm^{3,}$ respectively. The loam soil sample volume was 300 ml and 350 ml for the SKU: SEN0193 and SKU: SEN0308 sensors, respectively. The bulk density of the used loam soil sample was estimated at 1.114 g/cm^3 and 1.244 g/cm^3.

In this experiment, the data from SKU: SEN0193 and SKU: SEN308 sensors were measured using an Arduino UNO and recorded in an Excel file. Data was collected within 2-4 mins after inserting the sensor in the sample and recorded when the sensors started giving a stable voltage reading. Initially, the output Voltage from the sensors was recorded as the data and then plotted with the actual VWC calculated from the gravimetric moisture content of the soil sample. Then the Voltage was converted to measured VWC from the linear and 2nd order polynomial equations, which was developed by plotting the sensor voltage reading on the x-axis against the actual VWC on the y-axis. For this experiment, eighteen DFRobot capacitive soil moisture sensors were used where nine of them being SKU: SEN0193 and the other nine being waterproof SKU: SEN0308 model. During the first calibration stage, the sensor voltage reading for air and water was noted to check the variability of the sensor. It was found that the sensor had their unique qualities as they provide a different reading in the air and water.

3.4 Evaluation of sensors performance

The performance of the sensors was evaluated in various types of soil samples at different water contents. For this reason, a statistical analysis was done to determine how well the sensor predicts the real VWC based on the linear and second-order polynomial calibration equation. The mean absolute deviation (MAD) is one of the most important tools for determining how close the actual and predicted sensor readings are in an experiment. Therefore, the MAD was used to quantify the accuracy of predicted data compared to the actual values. In an experiment, Doležal et al. (2008) used average absolute deviations for soil moisture sensors by subtracting the actual water content in the soil and the predicted moisture content. The following equation (7) describes the MAD calculation:

$$MAD = \frac{1}{n}\sum_{i=1}^{n} |Actual\, VWC - Measured\, VWC| \tag{7}$$

Another method that has been used in different soil moisture-related studies (Bogena et al. 2007; Entekhabi et al. 2010; Moazenzadeh et al. 2022) is a root mean square error (RMSE), which is commonly used in modeling to measure the difference between the actual VWC values and the predicted VWC values. It depicts the sample's standard deviation in observed values and the predicted values determined using the calibration equations. Because the RMSE is a measurement that relies on the scale, it can reliably be used to estimate the accuracy of the models. The following equation (8) is used to calculate the RMSE:

$$RMSE = \sqrt{\frac{1}{n}\sum_{i=1}^{n}(Actual\ VWC - Measured\ VWC)^2} \quad (8)$$

The coefficient of determination, abbreviated as R^2, is the metric used to assess how effectively a statistical model predicts values compared to the actual data. In most cases, it is believed that a model is more accurately represented by having greater R^2 values. The R^2 values fall anywhere from +1 to -1, where the positive sign indicates the positively significant and the negative sign indicates the negatively significant.

3.5 Results and discussion

3.5.1 Calibration equations for soil moisture sensors

The initial sensor voltage reading in air and water, maintaining the same wiring, and operating on the same voltage supplies. For this reason, it is essential to calibrate each sensor before setting them in the field to measure soil moisture accurately. The sensor reading in the SKU: SEN0193 ranges from 2.57±0.049V in the air and 1.17±0.009V in the water, respectively. Similarly, the air voltage reading in the SKU: SEN0308 varied from 2.97±0.06V, while the water reading varied from 0.023±0.066V, respectively.

The sensor response variability indicates that their accuracy is inconsistent and fluctuates in each sensor. Considering this variability, a rigorous calibration is needed based on the soil types. The sample voltage reading was taken for each moisture-adjusted sample using SKU: SEN0193 and SKU: SEN0308 sensors for all three soil types until the soil became completely wet. The linear trendline was fitted to develop the calibration equation for each soil type. Fig. 3.2 depicts the linear and 2nd order polynomial fit with the SKU: SEN0193 sensors reading and the actual VWC reading calculated from the gravimetric water content of the sample soil. The actual VWC of the three soil types, sand, clay, and loam, ranged from 0.05 to 0.254 cm^3/cm^3, from 0.043 to 0.331 cm^3/cm^3, and from 0.145 to 0.382 cm^3/cm^3, respectively, for the samples used for the SKU: SEN0193 sensors.

On the other hand, Fig. 3.3 shows the linear and 2nd order polynomial fit with the SKU: SEN0308 sensors voltage reading and the actual VWC reading of the sample soil. The actual VWC for the sample soil used for SKU: SEN0308 sensors for the three soil types, sand, clay, and loam, ranged from 0.062 to 0.194 cm^3/cm^3, from 0.07 to 0.348 cm^3/cm^3, and from 0.097 to 0.294 cm^3/cm^3. Interestingly, the calibration equations from SKU: SEN0308 showed a variation in all these three types of soil. As both the SKU: SEN0193 and SKU: SEN0308 sensors operate in low frequencies and have sensitivity issues, the high mineral content may be the reason for reading variation in different soil (Bogena et al. 2017; Kizito et al. 2008; Nagahage et al. 2019).

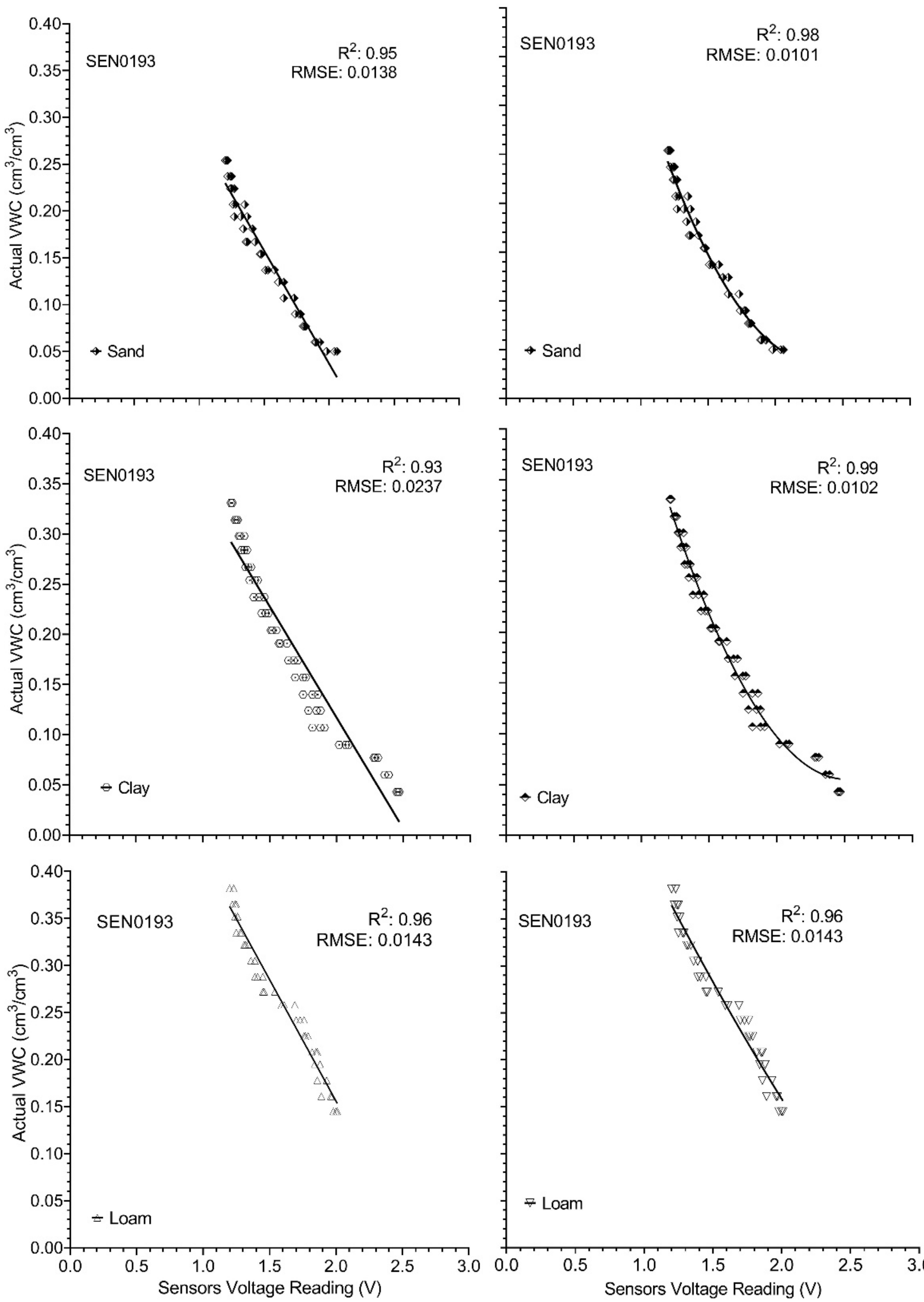

Fig. 3.2 Linear and 2nd order polynomial fit between the sensors voltage readings and the volumetric water content using the SKU: SEN0193 sensors from the sample sand, clay, and loam soil.

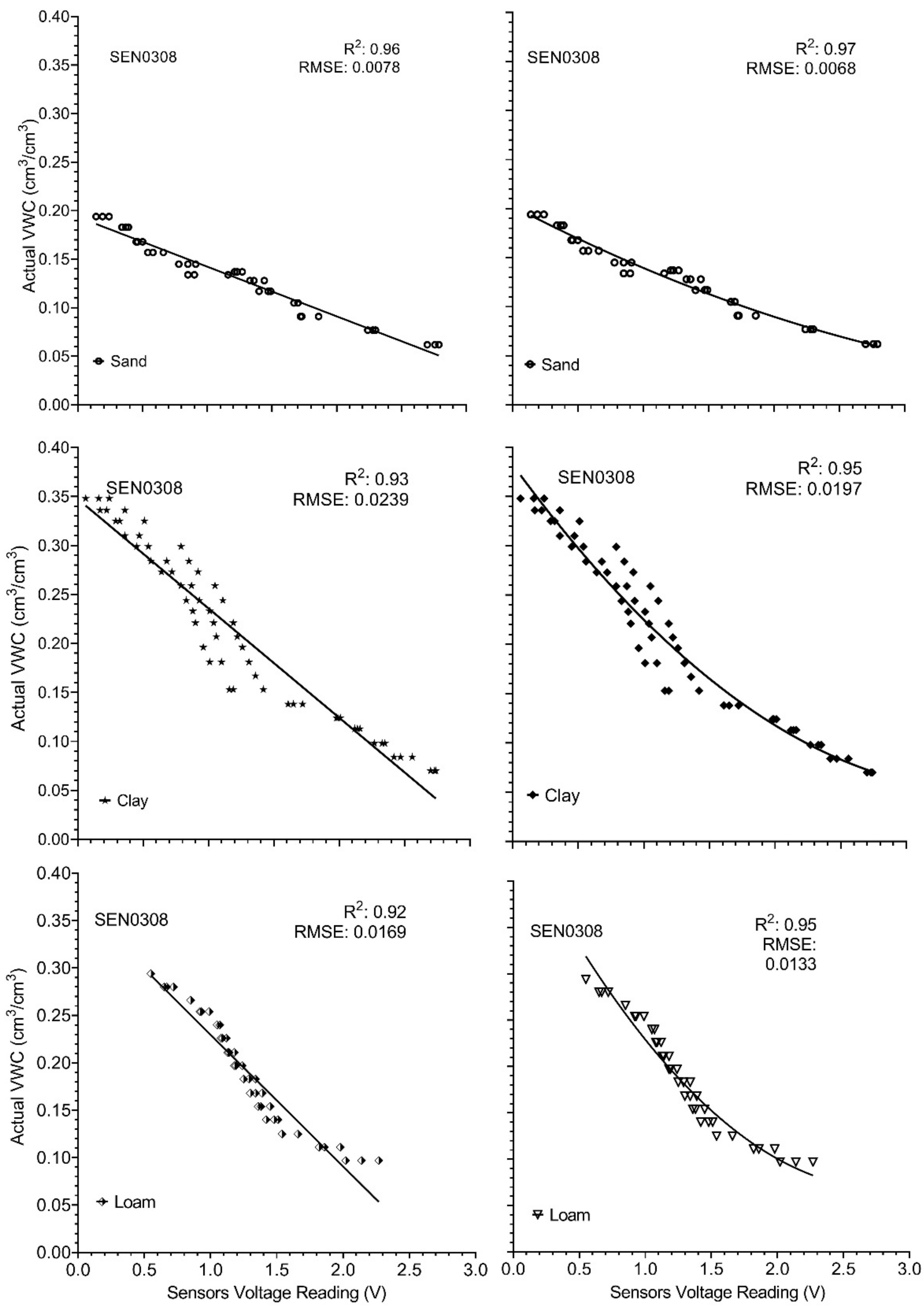

Fig. 3.3 Linear and 2nd order polynomial fit between the sensors voltage readings and the volumetric water content using the SKU: SEN0308 sensors from the sample sand, clay, and loam soil.

Table 3.1 Calibration equations, correlation coefficient (R^2), mean of absolute deviations (MAD), and root-mean-square errors (RMSE) between sensors voltage readings and the volumetric water content (VWC) in the sand, clay, and loam soil using the (a) SKU: SEN0193 and (b) SKU: SEN0308 sensors.

Sensor Types	Soil Types	Calibration Type	Calibration Equations	R^2	MAD	RMSE
	Sand	Linear	$Y = -0.2412*X + 0.5193$	0.96	0.011	0.0138
		2nd Order Polynomial	$Y = 0.1635*X^2 – 0.7597*X + 0.9191$	0.98	0.008	0.0101
SKU: SEN0193	Clay	Linear	$Y = -0.2215*X + 0.5601$	0.93	0.020	0.0237
		2nd Order Polynomial	$Y = 0.1572*X^2 – 0.7911*X + 1.051$	0.99	0.008	0.0102
	Loam	Linear	$Y = -0.2583*X + 0.6725$	0.96	0.012	0.0143
		2nd Order Polynomial	$Y = 0.0281*X^2 – 0.3478*X + 0.7416$	0.96	0.012	0.0143
	Sand	Linear	$Y = -0.0511*X + 0.1935$	0.96	0.006	0.0078
		2nd Order Polynomial	$Y = 0.0066 *X^2 – 0.0697*X + 0.2026$	0.97	0.005	0.0068
SKU: SEN0308	Clay	Linear	$Y = -0.1115*X + 0.3474$	0.93	0.018	0.0239
		2nd Order Polynomial	$Y = 0.0252*X^2 – 0.1826*X + 0.3824$	0.95	0.014	0.0197
	Loam	Linear	$Y = -0.1389*X + 0.3685$	0.92	0.013	0.0169
		2nd Order Polynomial	$Y = 0.049*X^2 – 0.2756*X + 0.4557$	0.95	0.011	0.0133

The derived soil-specific linear calibration equations and 2nd order polynomial equations were used to convert the sensor voltage reading to VWC measured by the sensors. All the sensor voltage readings from SKU: SEN0193 and SKU: SEN0308 were converted to VWC using the equations in Table 3.1. The major contrast between the performance of the two types of sensors shows that both sensors reading is closed to the actual VWC. The SKU: SEN0193 sensors seem better in clay soil compared to the SKU: SEN0308 sensors.

3.5.2 Comparison of actual VWC and sensor measured VWC

The R^2 values for the sand, clay, and loam soil samples were 0.96, 0.93, and 0.96 in the linear equations, whereas 0.98, 0.99, and 0.96 in the 2nd order polynomial equations. The RMSE values in SKU: SEN0193 sensor was 0.0138 cm^3/cm^3, 0.0237 cm^3/cm^3, and 0.0143 cm^3/cm^3 in linear calibration and 0.0101 cm^3/cm^3, 0.0102 cm^3/cm^3, and 0.0143 cm^3/cm^3, respectively (Fig. 3.4 and Table 3.1). From the fit by the x and y scatterplot, it is evident that most of the VWC values converted from the voltage reading measured by the sensor were closely aligned with the 45° reference identity line, indicating the reading is very close to the actual VWC. Similarly, the R^2 values for sand, clay, and loam soil sample were 0.96, 0.93, and 0.92 in the linear equation, while 0.97, 0.95, and 0.95 were in the polynomial calibration equations, respectively. At the same time, the RMSE values calculated using the SKU: SEN0308 calibration equations were 0.0078 cm^3/cm^3, 0.0239 cm^3/cm^3, and 0.0169 cm^3/cm^3 in the linear calibration and 0.0068 cm^3/cm^3, 0.0197 cm^3/cm^3, and 0.0133 cm^3/cm^3, in the polynomial calibration, respectively (Fig. 3.5 and Table 3.1).

Similarly, in the SKU: SEN0193 sensor, the values were close to the 1:1 line when plotting the actual VWC and measured VWC (Fig. 3.5). The Actual VWC ranged from 0.151±0.064 cm^3/cm^3, 0.188±0.088 $cm^3/cm^{3,}$ and 0.265±0.074 cm^3/cm^3 for sand, clay, and loam, respectively while the sensor SKU: SEN0193 predicted VWC ranged 0.151±0.063 cm^3/cm^3, 0.188±0.085

cm^3/cm^3, and 0.264±0.072 cm^3/cm^3 in linear and 0.151±0.063 cm^3/cm^3, 0.188±0.088 cm^3/cm^3, and 0.265±0.072 cm^3/cm^3 in polynomial for the same soil samples.

Likewise, the actual VWC for the sand, clay, and loam soil samples ranged from 0.131±0.039 cm^3/cm^3, 0.212±0.088 cm^3/cm^3, and 0.189±0.058 $cm^3/cm^{3,}$ while the predicted VWC from the sensor voltage reading using linear calibration equation was ranged 0.131±0.038 cm^3/cm^3, 0.212±0.084 cm^3/cm^3, and 0.188±0.056 cm^3/cm^3. The measured VWC by the 2^{nd} order polynomial equations were 0.131±0.038 cm^3/cm^3, 0.212±0.086 cm^3/cm^3, and 0.188±0.057 cm^3/cm^3. The predicted VWC by the sensors appears nearly identical to the actual VWC.

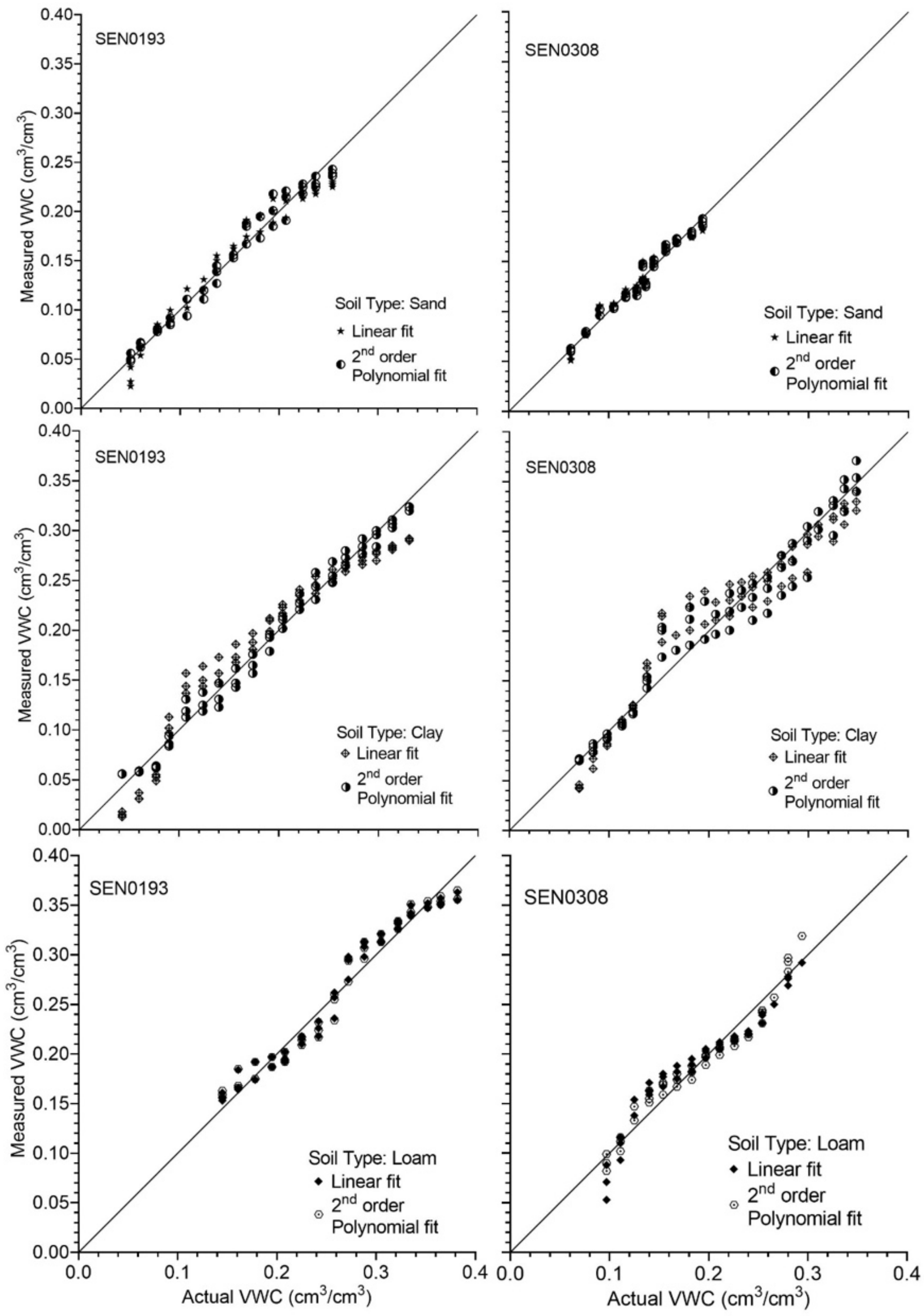

Fig. 3.4 Linear and 2nd order polynomial fit between the actual VWC and the measured VWC converted using the calibration equation created for the sensors from the sand, clay, and loam soil.

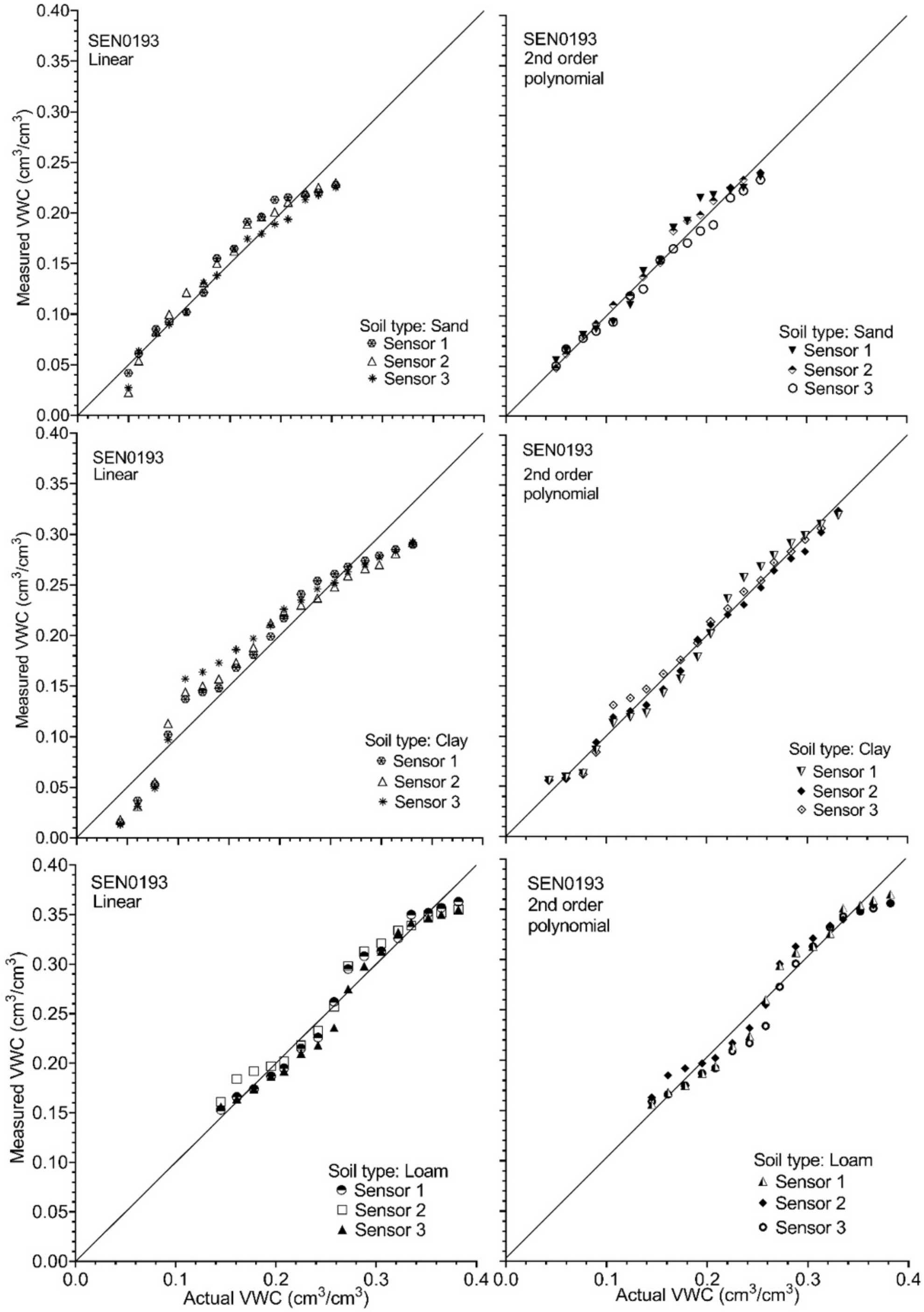

Fig. 3.5 Sensor to sensor reading variations and their fit with the line of identity where the actual VWC and the measured VWC converted using the linear equations from the sand, clay, and loam soils for sensor SKU: SEN0193.

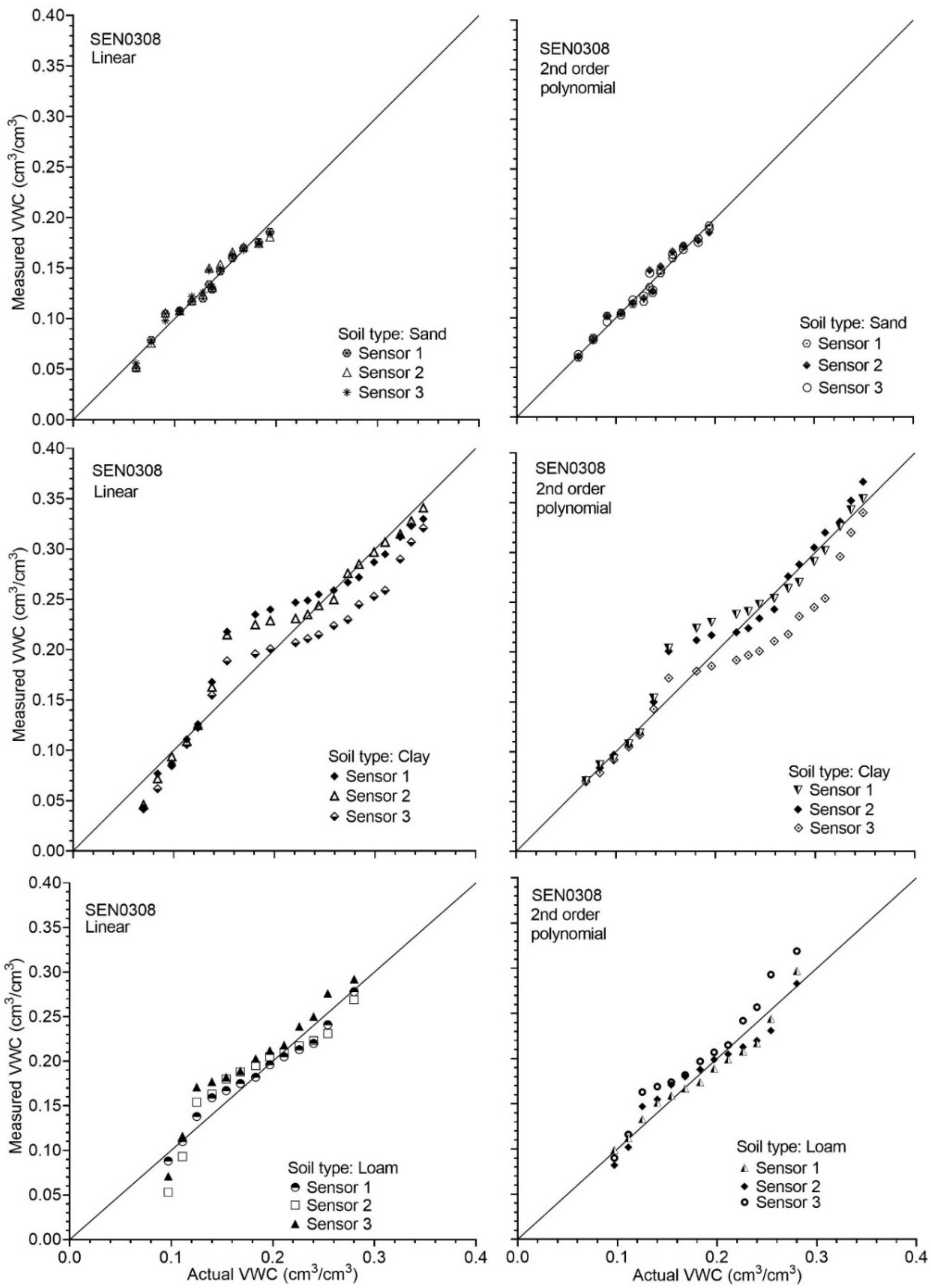

Fig. 3.6 Sensor to sensor reading variations and their fit with the line of identity where the actual VWC and the measured VWC converted using the linear equations from the sand, clay, and loam soils for sensor SKU: SEN0308.

3.6 Conclusions and recommendations

Accurate measurement of soil moisture content in the field is essential for better crop growth and irrigation decisions. This study aimed to calibrate the DF Robot low-cost capacitive soil moisture sensor (SKU: SEN0193 and SKU: SEN0308) that could be used in the field to measure the volumetric water content accurately. The calibration was performed in the lab to demonstrate the sensors' performance in different and replicated soil samples under controlled conditions. There was a variation in the sensors' response to the air and water voltage readings. The soil-specific linear and 2nd order polynomial calibration equations for sand, clay, and loam for the sample soil and their performance were satisfactory. Although both calibrations were a good fit, using the 2nd order polynomial is recommended as it covers more sensor values and is closer to the actual VWC than the linear equation. In addition, the linear calibration showed that the VWC and sensor voltage reading generated by the sensors has an R^2 of 0.96, 0.93, and 0.96 for sand, clay, and loam in SKU: SEN0193 and 0.96, 0.93, and 0.92 using the SKU: SEN0308 sensor for the same types of soil sample under the same lab conditions. The 2nd order polynomial equations performed better with the R^2 of 0.98, 0.99, and 0.96 for sand, clay, and loam in SKU: SEN0193 and 0.97, 0.95, and 0.95 using the SKU: SEN0308 sensor for the same soil samples. The findings show that the capacitive soil moisture sensors could be a viable device for measuring and monitoring VWC in sand, clay, and loam soil. As the soil depth range of these sensors differed, the SKU: SEN0308 sensor seems more reliable than the SKU: SEN0193, considering the former sensor covers better soil depth. It was particularly noticeable that the SKU: SEN0193 and SKU: SEN0308 sensors were not as good in clay soil compared to other soil types. Furthermore, it is strongly recommended to calibrate each sensor before installing them in the field.

Chapter 4 Design and evaluation of a plant-controlled atmometer for measuring crop evapotranspiration

4.1 Abstract

Irrigation is essential for optimal crop development and yield enhancement. Atmometers measure the evaporation rate through a porous surface to estimate the potential evapotranspiration (ET_p), which is used to calculate the actual crop water consumption (ET_a) using crop coefficients. When the soil is dry, however, plants transpire at a lower rate due to the increasing difficulty in drawing water from the soil. Therefore, the ET of a plant spans two phases: weather limiting Phase 1 and soil limiting Phase 2. The traditional atmometers presume that the crop is adequately irrigated and do not account for the drop in evapotranspiration caused by drier soils as in Phase 2. The objective of this project was to design and evaluate a plant-controlled atmometer capable of detecting crop water ET under both Phases 1 and 2. An atmometer with a variable evaporation rate determined by weather conditions and soil water status was built and tested. Experiments on the rate of evaporation through porous plates revealed that evaporation could be controlled by imposing a negative pressure on the water supply side to mimic the plants. Evaporation rates through porous ceramic plates were measured under different negative pressures to develop a relationship. This relationship was used to simulate the plant ET under different soil water contents and regulate the evaporation rates through the modified atmometer based on soil water content. In this experiment, an increase in ET rate led to increased negative pressure on the water supply side when the water supply was restricted. Water was released from the reservoir to the porous ceramic plate to match the weather conditions and the soil water content to mimic the plant. The change in water volume in the supply reservoir was used to calculate the ET_a of the crop.
Keywords: Atmometer, Evapotranspiration, Evaporation rate, Soil moisture sensors, Irrigation scheduling

4.2 Introduction

Irrigation scheduling refers to the precise amount and timing of water application in the field. A criterion is used to evaluate irrigation requirements, and a strategy is used to specify how much water to release under every condition (Broner 2004; Irmak, Payero, et al. 2005). It is also vital to understand the water requirements of different crops to provide efficient irrigation planning. Since the need for water fluctuates between crops, depending on weather and crop diversity. Measuring the overall irrigation needs in various agricultural growth phases is also vital (Bacci et al. 2008; Villaroman et al. 2018).

For a sustainable agricultural operation, it is essential to irrigate the crops by determining the crop water requirements. The crop water requirement can be measured in different ways, like lysimeters, pan evaporation, and atmometers. One of the most commonly used devices, called an atmometer, has been used to measure the rate of evaporation affected by weather conditions. The evaporation rate is then converted to crop evapotranspiration (ET) with an appropriate crop co-efficient (Irmak, Dukes, et al. 2005). Traditionally, atmometers respond to vapour pressure with humidity, solar radiation, and wind velocity variations. The atmometer assumes a well-watered field condition while predicting the ET of the plant using the evaporation rate and crop coefficients. However, the ET of the plants decreases with the reduction of the soil water content in the field. The evaporation rate through the meniscus relies on the pressure difference between the atmosphere and water pressure in the supply reservoir. Therefore, the ET during the soil limiting stage can be mimicked by controlling the negative backpressure on the reservoir side (Sri Ranjan 2012).

Over the last several decades, technological developments have significantly improved crop yield in sustainable agriculture. A general improvement was observed, starting with the enhancement of the tillage operation, fertilizer application, irrigation, and drainage (Rose et al. 2015; Sayre and Hobbs 2004; Siddique et al. 2012). By promoting intelligent technologies such as the internet of things (IoT), the automation of agricultural operations is increasing rapidly(Kadam and Rajashekarappa 2018).

The IoT refers to physical devices connected to the internet that is incorporated with various sensors, software, and data collection and transmission technologies. This is a cost-effective tool for transmitting real-time data without the involvement of humans in a variety of operations (Ashraf and Chowdhury 2022; Kale and Sonavane 2019; Mahbub 2020; Roy et al. 2019). With the integration of IoT with irrigation scheduling, a greater amount of water savings and proper irrigation management can be achieved (Ayaz et al. 2019; Elijah et al. 2018; Rajaram and Sundareswaran 2020; Roy et al. 2021).

To improve the accuracy and minimize over-irrigation, a newly designed plant-controlled atmometer is necessary. The main objective of this study was to develop and evaluate real-time irrigation scheduling using a plant-controlled atmometer and IoT. A plant-controlled atmometer that accurately measures the crop water requirement is built and field tested. The plant-controlled atmometer can be used for real-time irrigation scheduling using IoT to share the field data directly with the farmer using a cellular phone for making irrigation decisions.

4.3 Materials and methods

The development of the plant-controlled atmometer was divided into two steps. The first step was determining whether the evaporation rate varies with different negative pressure heads. The second step of the project involved laboratory work, including designing and selecting different parts of the systems. In addition, testing and calibrating the various sensors became essential for the project. Several sensors and IoT devices were evaluated before the selection of the different components for this project. The major components used in this experiment are listed in Fig. 4.1.

(a) Arduino MKR GSM 1400

(b) Solenoid Valve

(c) Honeywell Pressure Sensor

(d) DFRobot Waterproof Capacitive Sensor

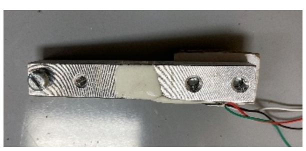

(e) 10kg Load Cell

(f) Arduino UNO

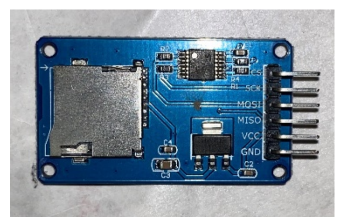

(g) Arduino SD Card Module

Fig. 4.1 Microcontroller and sensors used in the programming of plant-controlled atmometer

4.4 Determining evaporation rates under different negative pressures

This apparatus consisted of a ceramic plate that was connected to a metal pipe using a funnel and an O ring. A Tygon tube ¼ inch in diameter and about 2 m in length was connected to the metal pipe and filled with water to check whether it was completely sealed. Afterward, a 100 ml (about 3.38 oz) burette was connected to the other end of the Tygon tube to measure the water lost by evaporation through the porous ceramic plate. Three identical setup were built to collect data with replication. In the beginning, the height of the ceramic plate and the burette water level were kept at the same height for one hour, and observed the level of evaporation as the volume changed in the burette. After one hour, the height of the burette was brought down 10 cm (about 3.94 in) to measure the change in the evaporation rate. In the next hour, the height of the burette was again adjusted and lowered another 10 cm (about 3.94 in), and the evaporation rate was recorded. The process was continued until a 100 cm negative pressure head was imposed on the porous ceramic plate. The diameter of the porous ceramic plate was measured to be 11.4 cm (about 4.49 in), and the area of the ceramic plate was 102.07 cm^2.

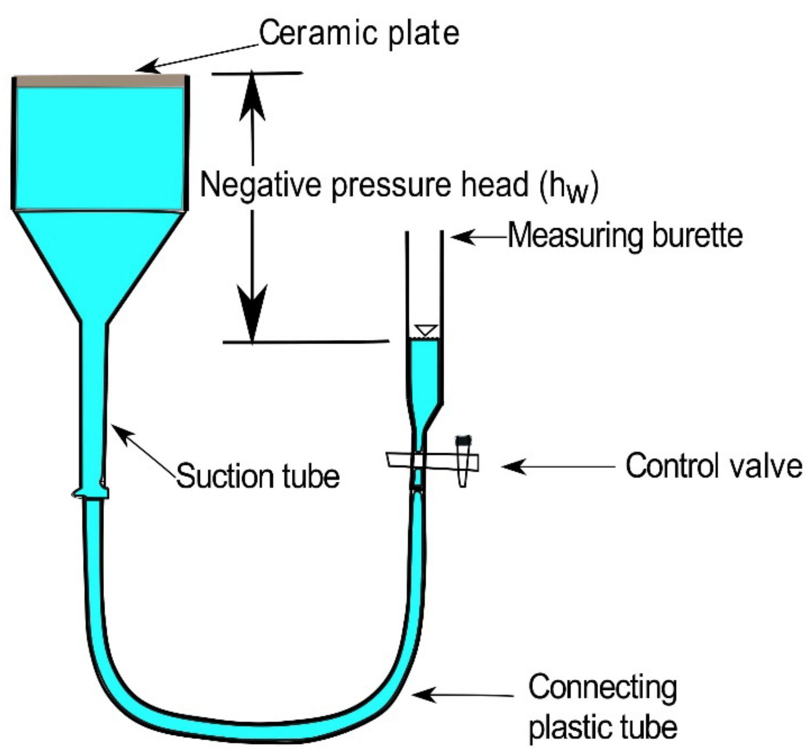

Fig. 4.2 Schematic illustration of the different parts of the atmometer for evaporation measurement under different negative pressure heads during calibration.

4.5 Design components of a plant-controlled atmometer

The plant-controlled atmometer was designed to enclose all the electronic parts of the system and reservoir in a wooden structure, as shown in Fig. 4.5. The selection of different components was based on the requirements, functionality, and performance in the preliminary tests. A pressure sensor was used to measure the negative pressure, a solenoid valve was used for controlling the water flow to the porous ceramic plate from the water reservoir, a load cell was used for measuring the weight of the water removed from the reservoir which was the same as the amount of water evaporated through the porous plate, and a soil moisture sensor was used to determine the soil moisture status. The descriptions of the different parts used in the experiment are given below:

In this experiment, a Brass Liquid Solenoid Valve (Geerte 2W-160-15, www.adafruit.com) was used to control the water flow from the reservoir to the porous plate. This solenoid valve has 1/2" (Nominal NPS) out and is usually a closed type of valve. The selected solenoid valve does not require any back pressure to run. The operating voltage for this valve is 12VDC, while the dimensions are 10.5 cm * 5.5 cm * 6.5 cm long with a weight of about 771 grams (g). A 12V 5A power adaptor was used to supply the power required by the solenoid valve. For the connection, control, and making of the solenoid functional with an Arduino board, a 5V relay module was used.

A Honeywell Differential Pressure sensor (26PCGFA6D, https://sps.honeywell.com) was used for measuring the pressure changes in the water supply side of the porous plate system due to evaporation through the porous plate. This sensor is an unamplified 0-250 psi pressure range sensor with a straight port and four pins. The advantage of the sensor is that it is a low-cost wet differential sensor capable of temperature compensation and calibration. This sensor operates in a temperature range of -40 to 85°C. The dimension of the sensor is 3.43 cm*1.27 cm* 0.79 cm. It can measure vacuum and positive pressure. An HX711 amplifier was used to amplify the sensor to get a the reading as psi, pascal, and atm output. The operating voltage of the sensor is 2.5V-16V, and the output accuracy for this sensor is ±0.7%.

A load cell is a device used to quantify strain in proportion to the applied load. When a load is applied to a strain gauge, it deforms and produces a voltage proportional to the applied load. This relationship between strain and voltage is used in various weight measurement applications. Load cells are commonly used because of their linearity, low cost, and ease of installation (Qandil and Zaid 2015). For this experiment, a 10kg load cell (SEN-13329, www.sparkfun.com) was used to quantify the water evaporation rate using the reservoir's weight change. An amplifier HX711, a 24-bit analog-to-digital converter that transforms the small strain changes from the load cell into 24-bit voltage changes in Arduino, was used. Load cells typically consist of four strain gauges connected in a Wheatstone bridge, which enables us to obtain accurate readings of the applied resistance. The operating voltage supply of a load cell is 2.6V-5.5V, and the dimension of the straight bar load cell is 8 cm * 1.27 cm * 1.27 cm. Calibration is a requirement before using a load cell. The calibration was performed with a known weight, and a calibration factor was noted for the final programming. The code was modified in the Arduino IDE, and the calibration factor was added for transforming the data from the load cell. As a result, the Arduino was able to resolve weight fluctuations as low as the load cell's range.

In this experiment, a DFRobot waterproof capacitive soil moisture sensor (SKU: SEN0308, https://www.dfrobot.com/) was attached to the plant-controlled atmometer. This sensor uses capacitive sensing rather than the more conventional resistive sensing for soil moisture monitoring. This sensor uses corrosion-resistant materials for long life. Burying the sensor within the root zone of the plants allows for collecting accurate, real-time information about soil moisture levels. This module has a built-in voltage regulator; thus, it can run between 3.3 and 5.5 volts. It worked well with 3.3V and 5V microcontrollers because of their low power requirements. The sensor has an operating current of 5 mA and an output voltage of 0–3.3 VDC. The sensor weight is only 15g, making it a lighter option. Equipment used in this study included a sensor, an Arduino UNO board, a breadboard, a digital scale, and connecting cables. Two of the most crucial characteristics, soil volume, and weight in both its wet and dry states, must be known to accurately calibrate the soil moisture sensor. These sensors were calibrated extensively, as described in chapter 3 of this thesis.

One of this experiment's most critical aspects was uploading the real-time sensor data to a cloud server. A microcontroller board capable of connecting with a cellular network was needed to upload the data to the cloud. For this reason, the Arduino MKR GSM 1400 (SARA-U201, www.arduino.cc) module was used in the lab to test the systems and upload the data. An Arduino UNO is low power-consuming device but incapable of cellular network connection. In the field experiment, it was used along with an Arduino SD card module to record the data in text format. Overall, the Arduino microcontroller was the center of all programming, uploading, and recording of the sensor data to the SD card for further analysis.

4.5.1 Wiring of the sensors with Arduino programming

In this experiment, all the sensors were connected to, and the programming code, was run on an Arduino IDE for uploading and verification. All the sensors were wired based on their power requirements. A breadboard was used to bridge all the connections between the sensors and the Arduino UNO board. The schematic wiring of the programming of different sensors used in the building of plant-controlled atmometer data logging system is shown in Fig. 4.3. The main programming code was written to consider the need and requirements of the output data from the sensors integrated with the systems. For this program to run, a logical flow was maintained for the sensors, and based on that, the microcontroller recorded the data in a 30 mins intervals from the sensors (Fig. 4.4). The Arduino Integrated Development Environment (IDE) lets the user write programs for microcontrollers in a language based on C/C++, test them, and upload them. During the individual sensor testing in the lab, the code for controlling each sensor was written. The sensor node program comprises several subroutines that are used to set up the microcontroller and other hardware parts, take measurements with the soil moisture sensor, load cell, and pressure sensor, and send sensor data to the microSD card. When the power adapters are first connected to the sensor node circuit to turn it on, the program starts by importing several external programming libraries. These libraries contain programmed instructions for different hardware functions.

After identifying the input and output pins of the microcontroller used in the circuit, the program variables were declared. The program then goes to the main routine and runs as long as the power is on. The main routine starts by calling separate subroutines that read the soil moisture sensor, the load cell, and the pressure sensor, switch on/off the solenoid, and then send sensor data. At the beginning of the program, the soil moisture sensor recorded the soil moisture status as a voltage output. The load cell recorded the weight changes of the water in the reservoir of the atmometer system. The pressure sensor recorded the negative pressure on the supply side of the porous ceramic plate. As the solenoid valve used in this experiment is a closed type, it remains shut, which means it does not allow water to pass from the reservoir to the porous ceramic plate. After that, by programming, the pressure sensor value was checked with the stored negative pressure value found in the initial laboratory calibration. If the pressure sensor value was greater or equal to any of the accumulated negative pressure values, the solenoid valve was turned on, allowing the water to flow for a few of seconds and completing the loop by recording the changed pressure data. If not, the solenoid valve remained closed and recorded the pressure sensor value into the MicroSD card. The solenoid valve remained on longer when the differential pressure was smaller. As the differential pressure increased, the solenoid opening time was shorter to supply less water to the porous ceramic plate, thus mimicking the plants. The data were recorded for the sensors to the MicroSD card every 30 mins. All the steps were repeated every 30 mins.

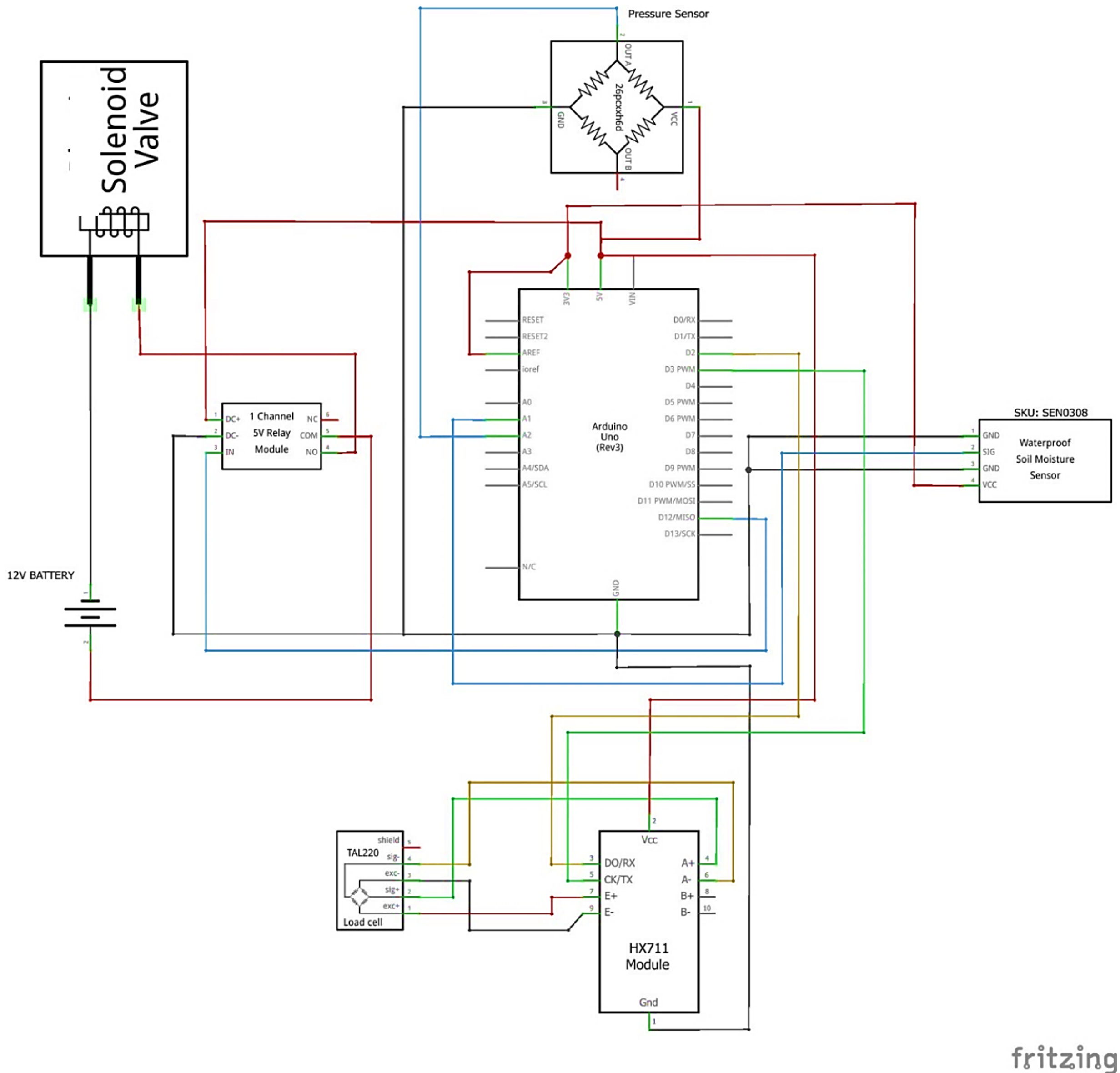

Fig. 4.3 Schematic of the programming of different sensors used in the building of plant-controlled atmometer and recording of the data from the sensors

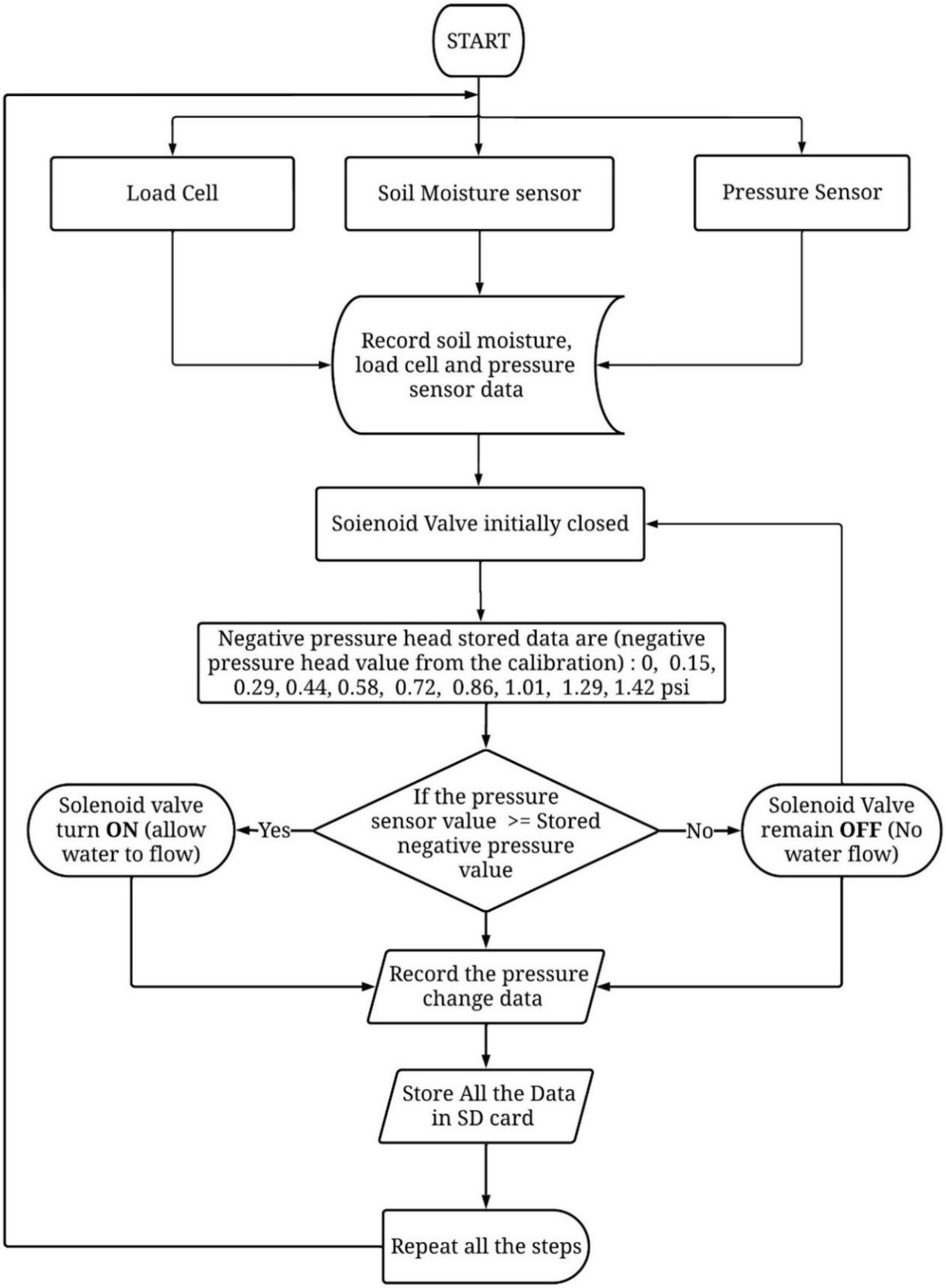

Fig. 4.4 Flow diagram of the programming flow, data accusation, and sensors performances integrated with the plant-controlled atmometer systems

4.5.2 Field setup of the plant-controlled atmometer

Three plant-controlled atmometer replicates were set up in the horticulture research field at the Point located at the Fort Garry campus of the University of Manitoba. The systems were installed at a similar elevations above the ground, and the capacitive soil moisture sensors were installed at 30 cm depths. The water reservoir of the system with an air inlet made with a rigid tube was maintained at the same height as the height of the ceramic plate of the system so that there was no gravity flow from the water reservoir to the ceramic plate. During the initial setup, air was removed from the systems by using a hand vacuum pump while keeping the ceramic place soaked in water. The replicates were installed about 40 cm from each other. All the wiring was checked and placed into a plastic box to keep it dry. The in-field setup of replicates and installation is shown in Fig. 4.5, and the schematic diagram of the system is shown in Fig. 4.6.

Fig. 4.5 In-Field setup and wiring of a plant-controlled atmometer

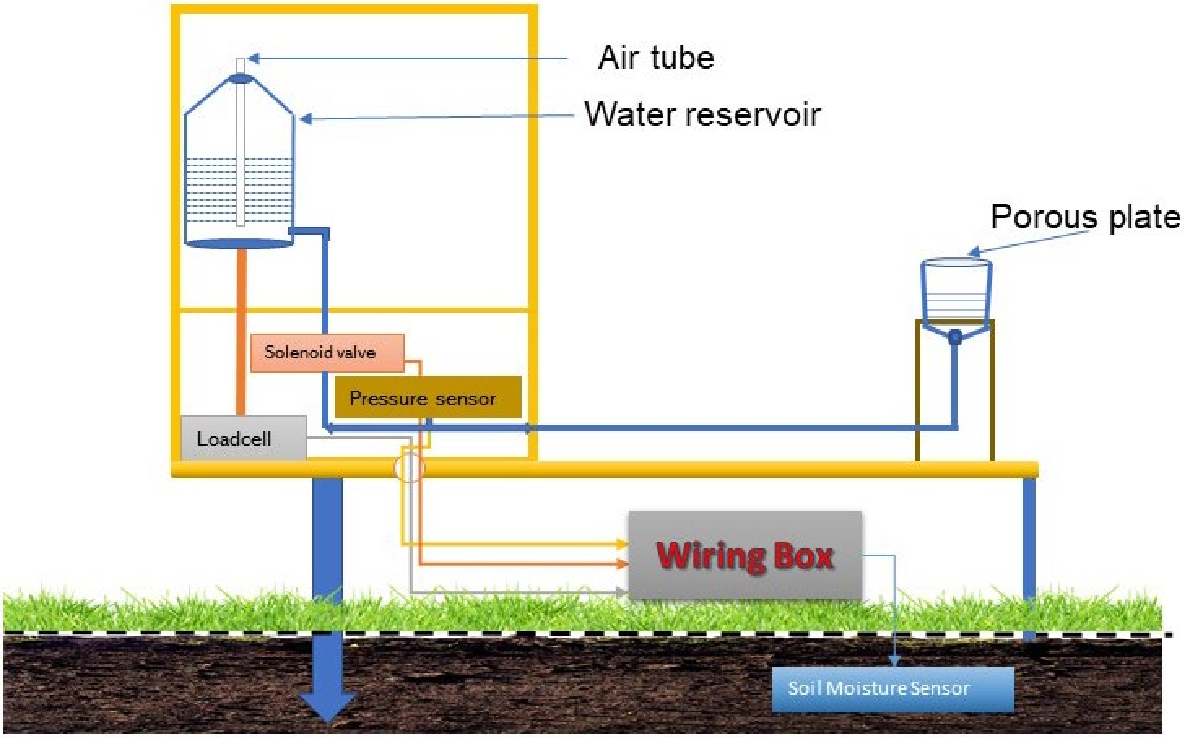

Fig. 4.6 Schematic of a Plant-Controlled Atmometer installation in the field condition

4.5.3 GSM module and Thingspeak

A Global Service Message (GSM) modem, also known as a GSM module, is a piece of hardware that utilizes the technology used in GSM mobile telephones to provide a wireless data connection to a cellular network. They identify their devices to the network via the use of SIM cards. With the help of the GSM library and the Arduino GSM shield, an Arduino board can connect to the internet, send and receive SMS messages, and make phone calls. Straight out of the box, the shield will be compatible with the Arduino Uno. There are two approaches to establishing a connection between Arduino and the GSM module through serial communication data transfers. The first approach is generally to connect the Tx pin of the GSM board to the Rx pin of the Arduino board and the Rx pin of the GSM module to the Tx pin of the Arduino.

The second method is to connect the Rx pin of the GSM module to the Tx pin of Arduino. The Arduino MKR GSM 1400 can interact with the help of cellular networks since it utilizes these networks. Due to the wide coverage of the GSM/ 3G network, GSM modules are a particularly appealing choice for connection in situations in which no other connectivity alternatives are available.

Ruby is the programming language used to create the open-source software called ThingSpeak. This software enables users to converse with internet-connected equipment. Providing an application programming interface (API) to both the devices and social network websites makes accessing, retrieving, and recording data more accessible. ThingSpeak enables quick visualizations of the data uploaded to the platform by connected devices. Because of ThingSpeak's capability of executing MATLAB® code, users can do real-time online processing and analysis of data. ThingSpeak has often been used in the prototype and proof of concept phases of Internet of Things (IoT) system development where analytics are involved. Through ThingSpeak, sensors, instruments, and websites can transmit data to the cloud, where it is either kept in a private or public channel. By default, data is stored in private channels inside ThingSpeak; however, public channels may be used to make data accessible to others. Cloud-based aggregation, visualization, and analysis of live data streams are all within reach when using the IoT analytics platform service provided by ThingSpeak. It is also possible to build quick visualizations of live data and issue warnings using ThingSpeak and transfer data sent from devices to ThingSpeak.

When carrying out this experiment, particularly the lab testing, real-time data upload, and visualization was achieved by creating a user account on the ThingSpeak website and logging into that account. A new data channel was created by selecting the field based on the identifying number of sensors and output required to be uploaded to the website. The metadata describing the data channel and the incoming data fields were added. The graphical result for each data field was customized as needed, displaying the data type, units, and time. After that, a one-of-a-kind numerical API key was produced for the data channel. This key was then used in the Arduino coding to upload the data. A channel number was assigned so users could visit the data channel's website. Subscribers can also designate the website as either private, in which case the user may only access it after successfully logging into their user account, or public, in which case anybody is allowed to view the graphical output of the webpage. A sample of the sensor data uploaded to the Thingspeak webpage is shown in Fig. 4.7.

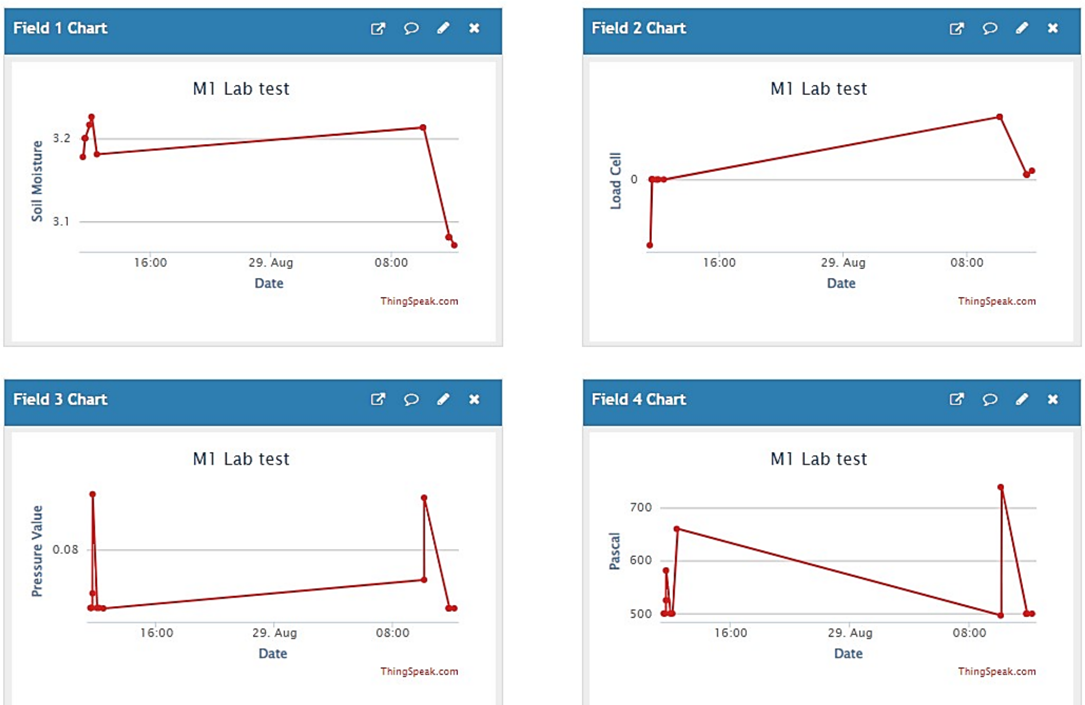

Fig. 4.7 A sample of the soil moisture sensor, load cell, and pressure sensor data uploaded to the ThingSpeak webpage

4.6 Results and discussion

The results of the experiment are presented in two parts. In the beginning, the evaporation rate was determined and calibrated. The calibration data is then used to write the programming code for the plant-controlled atmometer.

4.6.1 Calibration results of evaporation rate

The experiments for evaporation variation under different negative pressure heads were performed under ambient air pressure in a room with a constant temperature of 22°C at the Soil and Water engineering laboratory in the Department of Biosystems Engineering of the University of Manitoba. Among the three replicates, a similar trend was noticed that the evaporation rate decreased as the back pressure became increasingly negative.

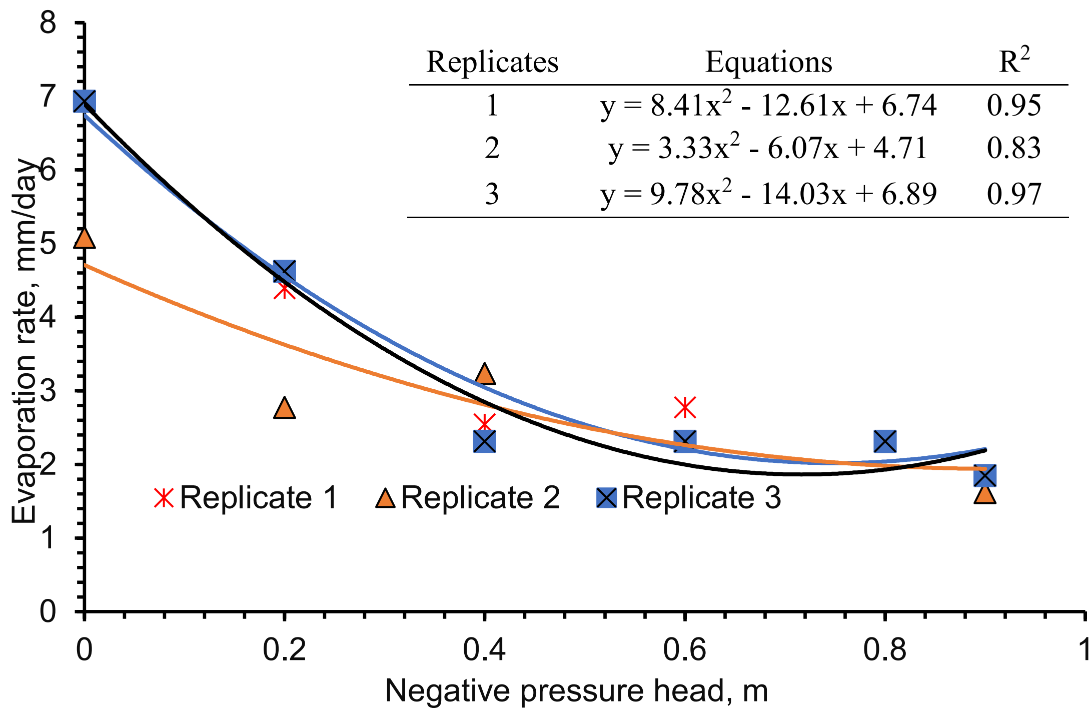

Fig. 4.8 Graphical representation of evaporation rate with a different negative pressure head of replicate 1, replicate 2, and replicate 3

In replicate 1 (Fig. 4.8), the evaporation rate was observed as 6.9 mm/day when no negative pressure was imposed. But when the negative pressure head was 0.9 m, the evaporation rate was 1.8 mm/day, which is the lowest in this system. Similarly, replicate 2 showed the highest evaporation rate (5.1 mm/day) at zero gauge pressure, while the minimum evaporation rate (1.6 mm/day) was observed at a negative pressure head of 0.9 m. Likewise, replicate 3 demonstrated a similar trend to the other two systems. The highest evaporation rate was 6.9 mm/day with 0 m negative pressure head, while at 0.9 m negative pressure head, the evaporation rate was 1.8 mm/day. It was also noticeable from the 2^{nd} order polynomial calibration equation that the R^2 values of the three replicates were 0.95, 0.83, and 0.97, respectively. The performance of replicate 2 was moderately low compared to the other two systems due to the possible leakage in the system. Thus, it clearly shows that the evaporation rate decreases with the increase in negative pressure head.

4.6.2 Temperature and rainfall on the experiment site

For the weather status in the field experiment, the weather station at the Point was located within 30 m. The temperature and rainfall data for the location were collected from the point weather station website (http://home.cc.umanitoba.ca/~grieger/weather.html). Maximum temperature, minimum temperature, average temperature, and average soil temperature was plotted along with the rainfall data during the experiment are shown in Fig. 4.9. As the experiment was carried out in late summer the average temperature was 14.84°C during the data collection period. The mean soil temperature of the experiment area ranged from 10.18°C to 18.65°C during the experiment. The Rainfall during the experiment was also higher than the usual weather conditions of the area. There was a severe rainfall event of about 25.4 mm during the experiment.

The soil type of the experimental field was heavy clay and the experiment was carried out in September, 2022.

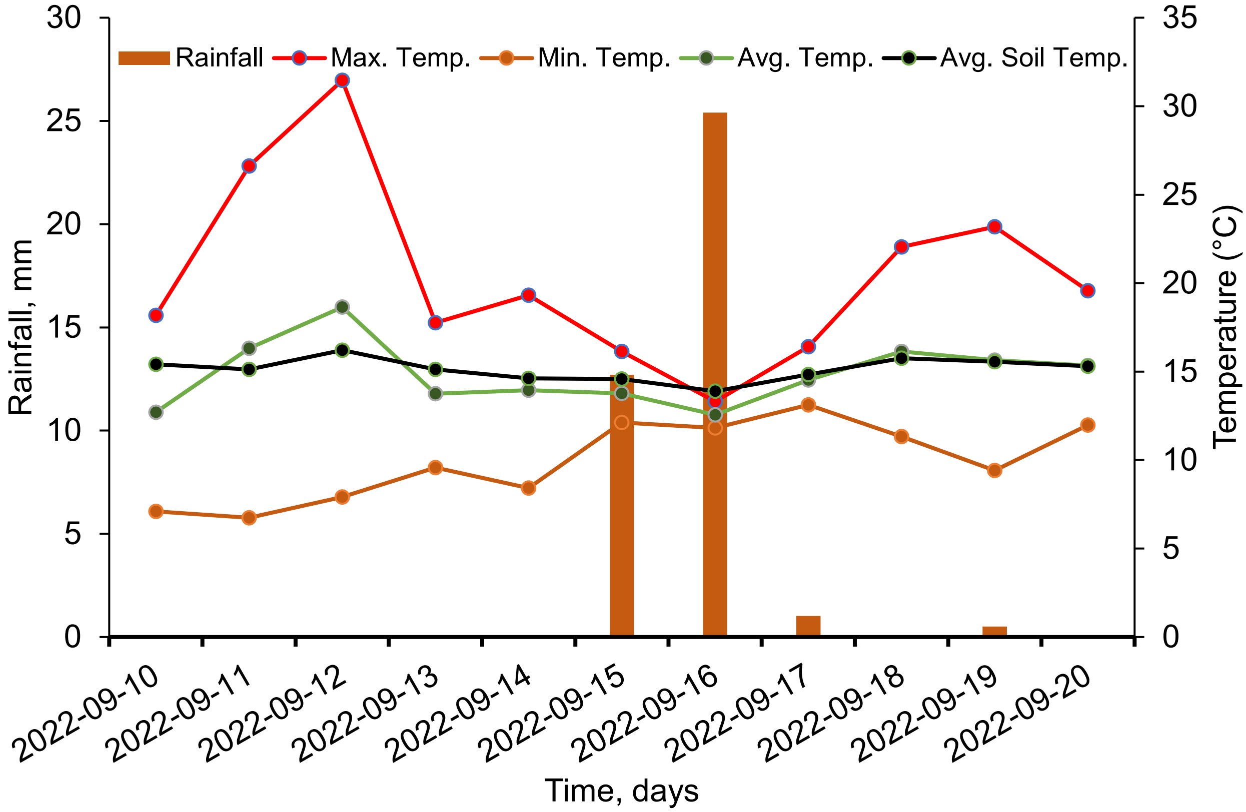

Fig. 4.9 Maximum temperature, minimum temperature, average temperature, average soil temperature, and daily precipitation data during the experiment.

4.6.3 Fields experiment results of plant-controlled atmometers

The field data was recorded and analyzed based on the performance of the three plant-controlled atmometers installed in the field. The data were recorded in text format on a MicroSD card. The text files were transferred into an Excel sheet to analyze the data. For analysis of the data, the capacitive soil moisture sensor data were recorded in voltage reading; the load cell data was recorded in grams, and the pressure sensor data was recorded in psi and pascal format.

4.6.3.1 Soil moisture sensor performance in the field

The soil moisture sensor voltage reading was recorded and converted into Volumetric Water Content (VWC) using a calibration equation. Fig. 4.10 shows the volumetric water content status of the experimental field and how different environmental parameters, such as rainfall, temperature, and, most importantly, grass, impacted the sensor reading. The average VWC ranged from 0.46±0.011 cm^3/cm^3. Noticeably, the figures show an increasing VWC reading during and after the rainfall in the field. The VWC measured in the experiment never exceeded the saturation point due to the heavy clay soil. This observation supports the clay soil moisture range of 40-60% (Kramarenko et al. 2016). In another study, the VWC for clay soil for a similar depth was over 40% (Kelleners et al. 2004). In an extensive calibration study for the soil moisture sensor, Rowlandson et al. (2013) observed that the soil texture and clay content greatly influenced the moisture level in clay soil. In this study, it was observed that all the soil moisture sensor was performed similarly. However, the soil moisture value range indicated a textural difference in the soil from the sensor-to-sensor installation locations.

4.6.3.2 Variations of ET rate in plant-controlled atmometer

The ET from the plant-controlled atmometer was calculated using the load cell data. The load cell recorded the weight of the water remaining in the reservoir continuously. It saved the recorded data into the microSD card. The data was then used to calculate the ET rate by dividing the weight difference between the load cell reading in grams converted to volume by the area of the ceramic plate of the atmometer the water evaporated. The recorded data was plotted using a moving trendline against the experiment time to observe the trend of the water evaporation rate from the systems. The variations in ET rate were distinct with the changing time (Fig. 4.10). The ET rate shows a steady performance based on the other weather parameters such as rainfall, air temperature, and wind speed. These systems show a higher ET rate with no rainfall but high temperature and wind speed. The influence of windspeed and temperature on the ET rate supported the findings of this experiment by multiple previous studies where it was stated that if the wind speed is higher, the ET rate will increase simultaneously (Davarzani et al. 2014; Igbadun et al. 2006). The evaporation rate on a rainy day is significantly lower than on a dry day (Irmak, Dukes, et al. 2005). The average ET rate was 0.46 mm/day, the maximum ET rate was 1.9 mm/day, while the minimum ET was 0.034 mm/day.

4.6.3.3 Performance of pressure sensor in the plant-controlled atmometer

The most significant aspect of this research is understanding how the pressure sensor responds to the changing ET rate and the different weather conditions. Another purpose of recording the pressure change data is to determine whether it mimics the ET with the changing negative pressure from the ceramic plate. The changing negative pressure values based on the soil moisture status in the field were found to be working according to our expectation (Fig. 4.10). Fig. 4.10 shows the results from single replicate. This replicate showed changes in pressure under different weather conditions. When there was no rainfall, the pressure reading was higher, while it decreased during rain events. These results support the patent held by Sri Ranjan (2012). The pressure changes in the plant-controlled atmometer ranged from 0-0.11 mH_2O. The reasons for not showing a significant difference were due to the cooler weather in September 2022. The weather during the experiment period was humid accompanied by lower air temperature leading to low evapotranspiration. Rainfall occurrences hampered the changes in pressure as the water was not evaporating enough from the systems. The figure also indicates a constant pressure for the first few days, and then pressure started to become more negative due to the reasonably dry days. The systems illustrate a fluctuation in pressure changes afterward due to frequent rain events. By the end, it shows an upward trend indicating the lower ET from the systems.

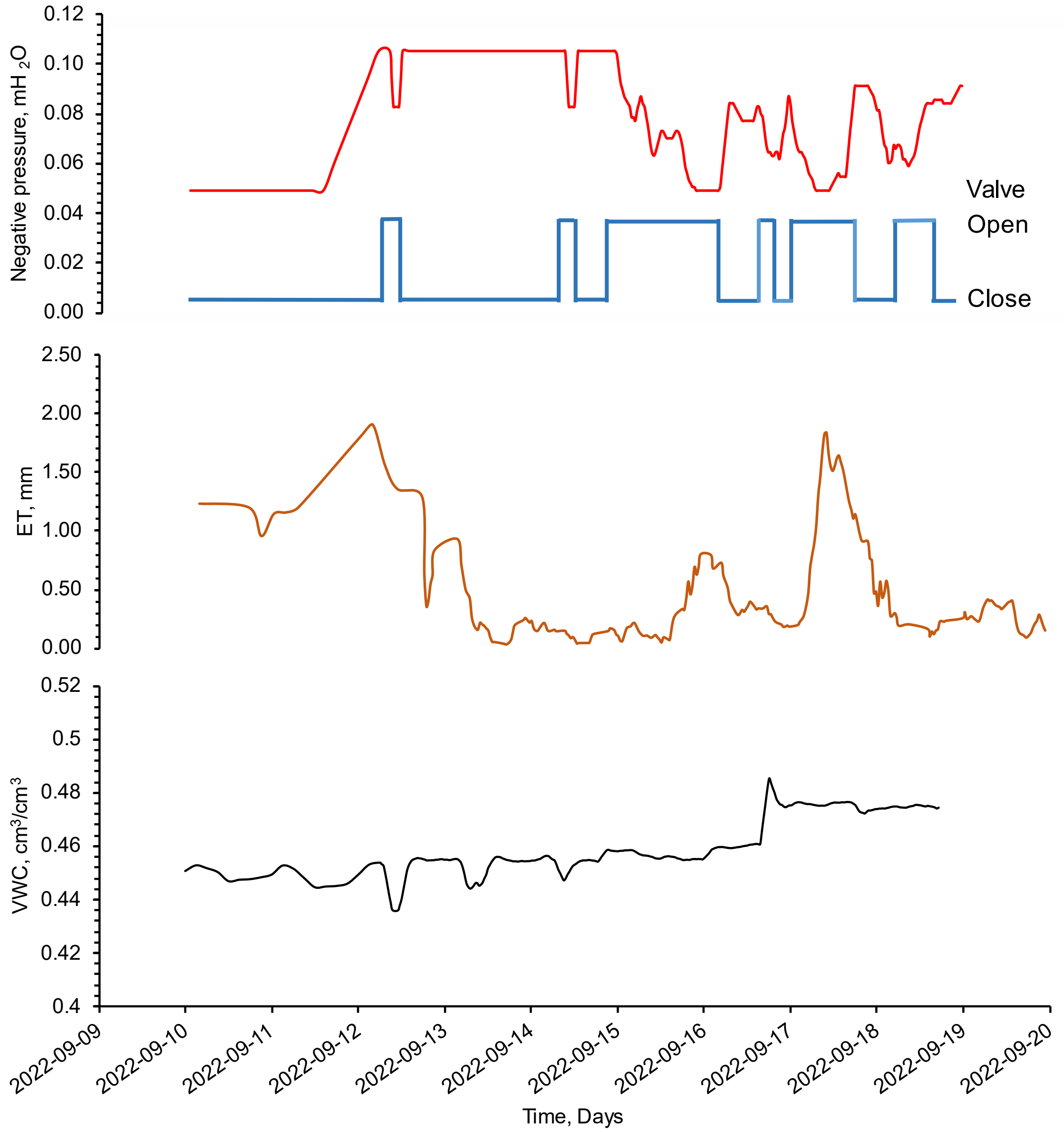

Fig. 4.10 Relationship among the pressure sensor response over time with evapotranspiration rate changes along with the soil moisture status changes in the plant-controlled atmometer system

4.6.3.4 Relationship among ET rate, negative pressure, and soil moisture data

Fig. 4.10 showed the relationship among the performances of different sensors in the system. The figure showed that the negative pressure was initially constant, and no changes were recorded. As the ET rate started to increase, the negative pressure on the water supply side of the ceramic plate increased rapidly initially, but when the ET starts decreasing, the negative pressure continues to rise slowly. After 2022-9-13, the ET rate started declining, which increased the negative pressure slowly. When the solenoid valve was allowed to release water, the ET rate started to increase while the negative pressure decreased. Due to the rain, the moisture content in the soil increased, simultaneously, the ET started rising due to the high wind, and the pressure decreased. The ET continued to decline as time passed, indicating that the pressure should be increased. This indicates that the solenoid valve remained closed to stop the water flow. The figure indicated that the ET changes proportionally with moisture content in the soil, and the pressure change was inverse. On 2022-9-17, the ET rate increased with increased soil moisture status due to heavy rain. These results support the idea of Dr. Sri Ranjan's patented technology that the crops ET rate is maximum when the soil is wet and characterized by the weather limiting phase, however, in the case of dry soil, it is difficult for the plant to draw water from the soil due to wilting (Sri Ranjan 2012).

4.7 Conclusions

The development of an accurate and precise plant-controlled atmometer will help the farmers to apply the correct amount of water required by the crop. Initially, the relationship between the negative pressure head and the evaporation rate was found to be significant. It was found that the higher the negative pressure head, the lower the evaporation rate. The coefficients of determination of polynomial regression between evaporation and negative pressure head were 0.95, 0.83, and 0.97, respectively. The soil water status also controlled the evaporation rate by altering the backpressure of the water supply side. Because of this relationship, the water evaporation rate measured by the atmometer can be adjusted to simulate the lower ET values that result from lower soil water content. A soil water content sensor placed within the crop root zone showed the potential to regulate the variation in the water evaporation rate connected with changes in ET that are generated by changes in soil water content. The plant-controlled atmometer was able to respond to both weather conditions and varying soil water status. It was able to better mimic the plant water use.

Chapter 5 Conclusions and recommendations

5.1 General conclusions

The research conducted in this study had three goals. The initial goal was to calibrate and assess the performance of two types of capacitive soil moisture sensors in different soil types. The sensor performance in various types of soil was recorded and analyzed based on sensor readings and the volumetric water content of the soil sample. The second goal was to construct and test a plant-controlled atmometer for measuring crop ET for irrigation scheduling. Furthermore, the performance of various sensors attached to the atmometer systems and how they interact with one another were monitored. It was also investigated whether the notion of managing ET by controlling water flow to the systems with the changing pressure recorded by a pressure sensor was viable. The coefficient of regression (R^2) and moving average trendline were employed in the statistical analysis. The key findings of the study are presented below.

5.2 Soil moisture sensors

The performance of the capacitive soil moisture sensor was evaluated to measure the soil moisture status in different types of soil (i.e., sand, clay, and loam) under different conditions. Based on the findings of the extensive calibration of the sensor, the sensors performed differently in different types of soil. The sensors values can be different from one another based on sample preparation and moisture present in the soil sample. The linear and 2nd order polynomial relationship between the sensor voltage reading and the gravimetric to volumetric converted reading fit well. The R^2 values were 0.96-0.98, 0.93-0.99, 0.96-0.96 for sand, clay, and loam soil for SEN0193 and 0.96-0.97, 0.93-0.95, 0.92-0.95 in SEN0308 sensors respectively. The fact that each sensor functions independently and needs to be calibrated before being installed in the field was one of the study's most important findings. It was also noticeable that the sensor performed differently in different types of soil. The soil-specific linear and 2^{nd} order polynomial calibration equations were satisfactory, but the 2^{nd} order polynomial showed a better performance.

5.3 Plant-controlled atmometer

The plant-controlled atmometer was designed and evaluated in the field to check the overall performance of the different sensors that formed the system. The performance of the sensors was considered satisfactory. The coefficients of determination of polynomial regression between evaporation and negative pressure head were 0.95, 0.83, and 0.97, respectively. The soil moisture sensor, load cell, and pressure sensor results showed a consistent trend when the moving average trendline was used. The soil moisture content was found to be 0.46±0.011 cm^3/cm^3. The consistency of the soil moisture data provides a clear understanding of the soil moisture status of the experiment field under different weather conditions. The evaporation from the porous ceramic plate was recorded, and a consistent trend was followed. The evaporation rate was higher on a non-rainy day and lowered on a rainy day. The systems recorded pressure changes with the increasing and decreasing trend of evaporation used here as a proxy for ET. The pressure changes range from 0-0.11 mH_2O. The average ET was found at 0.46 mm/day. The possibility to control the fluctuation in the water evaporation rate associated with variations in ET was demonstrated using a soil water content sensor positioned inside the crop root zone. This sensor could react to changing soil water status. The plant-controlled atmometer can be used to simulate plant water usage more accurately.

5.4 Recommendation for future study

Based on the study findings, some recommendations can be made for future studies. They are listed below:

i. This investigation highlighted the importance of sensor calibration before installation for monitoring soil moisture status. However, further long-term calibration in the field is necessary to ensure their long-term reliability in the area.

ii. Research must be undertaken to establish the optimal soil depth for monitoring soil moisture for irrigation scheduling, considering soil type and crop type, and adjusting the monitoring depth with the crop development stage.

iii. More research is needed to assess the efficacy of site-specific sensor calibration and its ability to minimize the ambiguity associated with determining the depth and duration of sensor installation.

iv. Growers must be instructed to interpret data ranging from raw sensor readings to soil moisture percentages.

v. Plant-controlled atmometers need to be tested under various weather conditions to monitor the changes in pressure and ET during weather change events.

vi. The power supply to the atmometer systems should be monitored to check the damage-prone sensors, such pressure sensor, solenoid valve, and soil moisture sensor.

vii. Plant-controlled atmometers should be installed in various crop fields to monitor the performance variation in different crop types.

List of References

Adelakun, I.A. and R. Sri Ranjan. 2013. Design of a multilevel TDR probe for measuring soil water content at different depths. *Transactions of the ASABE* 56(4): 1451–1460.

Adla, S., N.K. Rai, S.H. Karumanchi, S. Tripathi, M. Disse and S. Pande. 2020. Laboratory calibration and performance evaluation of low-cost capacitive and very low-cost resistive soil moisture sensors. *Sensors (Switzerland)* 20(2). https://doi.org/10.3390/s20020363.

Allen, R.G., M. Tasumi, A. Morse, R. Trezza, J.L. Wright, W. Bastiaanssen, W. Kramber, I.J. Lorite, et al. 2007. Journal of Irrigation and Drainage Engineering Satellite-Based Energy Balance for Mapping Evapotranspiration with Internalized Calibration (METRIC)—Applications. *Journal of Irrigation and Drainage Engineering* 133(4): 395–406. https://doi.org/10.1061/(ASCE)0733-9437(2007)133.

Allen, R., L. S. Pereira, D. Raes and M. Smith. 1998. FAO Irrigation and Drainage Paper No.56 Crop Evapotranspiration(Guidelines for Computing Crop Water Requirement). *Food and Agriculture Organization of the United Nations* 56(9): 26–40.

Ashraf, S. and A. Chowdhury. 2022. An Advanced Irrigation System Using Cloud-Based IoT Platform ThingSpeak. In *Cyber Security, Privacy and Networking*, 389–398. Springer.

Ashton, K. 2009. That ‘internet of things’ thing. *RFID Journal* 22(7): 97–114.

Asif, M., M. Ahmad, A.G. Mangrio, G. Akbar and A.H. Memon. 2015. Design, evaluation and irrigation scheduling of drip irrigation system on citrus orchard. *Pakistan Journal of Meteorology Vol* 12(23).

Ayaz, M., M. Ammad-Uddin, Z. Sharif, A. Mansour and E.-H.M. Aggoune. 2019. Internet-of-Things (IoT)-based smart agriculture: Toward making the fields talk. *IEEE Access* 7: 129551–129583.

Bacci, L., P. Battista and B. Rapi. 2008. An integrated method for irrigation scheduling of potted plants. *Scientia Horticulturae* 116(1): 89–97. https://doi.org/10.1016/j.scienta.2007.11.005.

Bierman, P.M. 2005. Managing irrigation for high-value crops.

Blanco, F.F., M. V. Folegatti, J.W. Knox, J.A. Rodriguez-Diaz, T.M. Hess, R. Fescue, I. Messing, K. Djaman, et al. 2004. Evaluation of evaporation-measuring equipments for estimating evapotranspiration within a greenhouse. *Revista Brasileira de Engenharia Agrícola e Ambiental* 8(2–3): 184–188. https://doi.org/10.1590/s1415-43662004000200004.

Blanco, F.F. and M. V. Folegatti. 2004. Evaluation of evaporation-measuring equipments for estimating evapotranspiration within a greenhouse. *Revista Brasileira de Engenharia Agrícola e Ambiental* 8(2–3): 184–188. https://doi.org/10.1590/s1415-43662004000200004.

Bogena, H.R., J.A. Huisman, C. Oberdörster and H. Vereecken. 2007. Evaluation of a low-cost soil water content sensor for wireless network applications. *Journal of Hydrology* 344(1–2): 32–42. https://doi.org/10.1016/J.JHYDROL.2007.06.032.

Bogena, H.R., J.A. Huisman, B. Schilling, A. Weuthen and H. Vereecken. 2017. Effective calibration of low-cost soil water content sensors. *Sensors* 17(1): 208.

van Brackel, J. 1980. Mass transfer in convective drying. *Advances in Drying* 1: 217–268. https://limo.libis.be/primo-explore/fulldisplay?docid=LIRIAS1925866&context=L&vid=Lirias&search_scope=Lirias&tab=default_tab&lang=en_US&fromSitemap=1

Broner, I. 2004. Irrigation Scheduling With Atmometers. *Colorado State University Extension, Fact Sheet No. 4.708* (4): 10–13. http://www.ext.colostate.edu/pubs/crops/04706.htm.

Broner, I. and R.A.P. Law. 1991. Evaluation of a modified atmometer for estimating reference ET. *Irrigation Science* 12(1): 21–26. https://doi.org/10.1007/BF00190705.

Brouwer, C. and M. Heibloem. 1986. Irrigation water needs. *Irrigation Water Management* Vol. 102(3): 1–40.

Brutsaert, W. 2013. Use of pan evaporation to estimate terrestrial evaporation trends: The case of the Tibetan Plateau. *Water Resources Research* 49(5): 3054–3058. https://doi.org/10.1002/wrcr.20247.

Campora, M., A. Palla, I. Gnecco, R. Bovolenta and R. Passalacqua. 2019. The laboratory calibration of a soil moisture capacitance probe in sandy soils. *Soil and Water Research* 15(2): 75–84. https://doi.org/10.17221/227/2018-SWR.

Chen, F. and P.J. Robinson. 2009. Estimating reference crop evapotranspiration with ETgages. *Journal of Irrigation and Drainage Engineering* 135(3): 335–342. https://doi.org/10.1061/(ASCE)IR.1943-4774.0000005.

Da Costa, E.F., N.E. De Oliveira, F.J.O. Morais, P. Carvalhaes-Dias, L.F.C. Duarte, A. Cabot and J.A. Siqueira Dias. 2017. A self-powered and autonomous fringing field capacitive sensor integrated into a micro sprinkler spinner to measure soil water content. *Sensors* 17(3): 575.

Das, S., T.S. Sarkar and B. Chakraborty. 2014. A semi-cylindrical capacitive sensor used for soil moisture measurement. *Int. Journal of Electrical, Robotics, Electronics and Comm. Engg.* 8(1).

Davarzani, H., K. Smits, R.M. Tolene and T. Illangasekare. 2014. Study of the effect of wind speed on evaporation from soil through integrated modeling of the atmospheric boundary layer and shallow subsurface. *Water Resources Research* 50(1): 661–680. https://doi.org/10.1002/2013WR013952.

Djaman, K., H. Tabari, A.B. Balde, L. Diop, K. Futakuchi and S. Irmak. 2016. Analyses, calibration and validation of evapotranspiration models to predict grass-reference evapotranspiration in the Senegal river delta. *Journal of Hydrology: Regional Studies* 8: 82–94. https://doi.org/10.1016/j.ejrh.2016.06.003.

Djaman, K. and S. Irmak. 2013. Actual Crop Evapotranspiration and Alfalfa- and Grass-Reference Crop Coefficients of Maize under Full and Limited Irrigation and Rainfed Conditions. *Journal of Irrigation and Drainage Engineering* 139(6): 433–446. https://doi.org/10.1061/(ASCE)IR.1943-4774.0000559.

Doležal, F., T. Litschmann, J. Kučera, J. Peterková, J. Zavadil, J. Vacek, P. Pražák, E. Pilná, et al. 2008. Field and laboratory ad hoc calibrations of Virrib and ThetaProbe dielectric sensors for soil moisture measurements. *Soil and Water Research* 3(4): 199–214. https://doi.org/10.17221/18/2008-SWR.

Du, Y.-J., N.-J. Jiang, S.-Y. Liu, S. Horpibulsuk and A. Arulrajah. 2016. Field evaluation of soft highway subgrade soil stabilized with calcium carbide residue. *Soils and Foundations* 56(2): 301–314.

Elanthiraiyan, P. and D.S. Babu. 2015. Smart medicine and physical health system using IoT. *International Journal of Computer Science and Mobile Computing* 4(3): 333–338.

Elijah, O., T.A. Rahman, I. Orikumhi, C.Y. Leow and M.H.D.N. Hindia. 2018. An overview of Internet of Things (IoT) and data analytics in agriculture: Benefits and challenges. *IEEE Internet of Things Journal* 5(5): 3758–3773.

Eller, H. and A. Denoth. 1996. A capacitive soil moisture sensor. *Journal of Hydrology* 185(1–4): 137–146. https://doi.org/10.1016/0022-1694(95)03003-4.

Entekhabi, D., R.H. Reichle, R.D. Koster and W.T. Crow. 2010. Performance Metrics for Soil Moisture Retrievals and Application Requirements. *Journal of Hydrometeorology* 11(3): 832–840. https://doi.org/10.1175/2010JHM1223.1

Eren, H. 2014. Capacitive sensors. *Measurement, Instrumentation, and Sensors Handbook: Spatial, Mechanical, Thermal, and Radiation Measurement* 1.

Evans, D. 2011. The internet of things. How the next evolution of the internet is changing everything, whitepaper. *Cisco Internet Business Solutions Group (IBSG)*.

Evett, S.R., A.W. Warrick and A.D. Matthias. 1995. Wall Material and Capping Effects on Microlysimeter Temperatures and Evaporation. *Soil Science Society of America Journal* 59(2): 329–336. https://doi.org/10.2136/sssaj1995.03615995005900020009x.

Fares, A. and V. Polyakov. 2006. Advances in crop water management using capacitive water sensors. *Advances in Agronomy* 90: 43–77.

Fu, G., S.P. Charles and J. Yu. 2009. A critical overview of pan evaporation trends over the last 50 years. *Climatic Change* 97(1): 193–214. https://doi.org/10.1007/s10584-009-9579-1.

Giambelluca, T.W., D.L. McKenna and P.C. Ekern. 1992. An automated recording atmometer: I. calibration and testing. *Agricultural and Forest Meteorology* 62(1–2): 109–125. https://doi.org/10.1016/0168-1923(92)90008-R.

Halliday, D., R. Resnick and J. Walker. 1993. Fundamentals of Physics Wiley. *New York*.

Hanson, B.R., S. Orloff and D. Peters. 2000. Monitoring soil moisture helps refine irrigation management. *California Agriculture* 54(3): 38–42. http://dx.doi.org/10.3733/ca.v054n03p38.

Ida, N. 2015. *Engineering Electromagnetics*. Springer.

Igbadun, H.E., H.F. Mahoo, A.K.P.R. Tarimo and B.A. Salim. 2006. Performance of Two Temperature-Based Reference Evapotranspiration Models in the Mkoji Sub-Catchment in Tanzania. *Agricultural Engineering International* 8: 1–19.

Irmak, S., J.O. Payero and D.L. Martin. 2005. Using Modified Atmometers (ET gage®) for Irrigation Management. *University of Nebraska–Lincoln Extension* G1579.

Irmak, S., M.D. Dukes and J.M. Jacobs. 2005. Using modified Bellani plate evapotranspiration gauges to estimate short canopy reference evapotranspiration. *Journal of Irrigation and Drainage Engineering* 131(2): 164–175. https://doi.org/10.1061/(ASCE)0733-9437(2005)131:2(164).

Irmak, S., J.O. Payero, D.L. Martin, A. Irmak and T.A. Howell. 2006. Sensitivity Analyses and Sensitivity Coefficients of Standardized Daily ASCE-Penman-Monteith Equation. *Journal of Irrigation and Drainage Engineering* 132(6): 564–578. https://doi.org/10.1061/(ASCE)0733-9437(2006)132:6(564).

Kadam, A.A. and Rajashekarappa. 2018. Internet of things in agriculture: A review. *Agricultural Reviews* (of): 32–36. https://doi.org/10.18805/ag.r-1836.

Kale, A.P. and S.P. Sonavane. 2019. IoT-based Smart Farming: Feature subset selection for optimized high-dimensional data using improved GA based approach for ELM. *Computers and Electronics in Agriculture* 161(April 2018): 225–232. https://doi.org/10.1016/j.compag.2018.04.027.

Kamaruddin, F., N.N.N. Abd Malik, N.A. Murad, N.M.A. Latiff, S.K.S. Yusof and S.A. Hamzah. 2019. IoT-based intelligent irrigation management and monitoring system using Arduino. *TELKOMNIKA (Telecommunication Computing Electronics and Control)* 17(5): 2378–2388.

Kaviany, M. and M. Mittal. 1987. Funicular state in drying of a porous slab. *International Journal of Heat and Mass Transfer* 30(7): 1407–1418.

Kazemi, M.A., D.S. Nobes and J.A.W. Elliott. 2017. Experimental and Numerical Study of the Evaporation of Water at Low Pressures. *Langmuir* 33(18): 4578–4591. https://doi.org/10.1021/acs.langmuir.7b00616.

Kelleners, T.J., R.W.O. Soppe, J.E. Ayars and T.H. Skaggs. 2004. Calibration of Capacitance

Probe Sensors in a Saline Silty Clay Soil. *Soil Science Society of America Journal* 68(3): 770–778. https://doi.org/10.2136/sssaj2004.7700.

Kizito, F., C.S. Campbell, G.S. Campbell, D.R. Cobos, B.L. Teare, B. Carter and J.W. Hopmans. 2008. Frequency, electrical conductivity and temperature analysis of a low-cost capacitance soil moisture sensor. *Journal of Hydrology* 352(3–4): 367–378. https://doi.org/10.1016/j.jhydrol.2008.01.021.

Kjaersgaard, J., R. Allen and A. Irmak. 2011. Improved methods for estimating monthly and growing season ET using METRIC applied to moderate resolution satellite imagery. *Hydrological Processes* 25(26): 4028–4036. https://doi.org/10.1002/hyp.8394.

Kojima, Y., R. Shigeta, N. Miyamoto, Y. Shirahama, K. Nishioka, M. Mizoguchi and Y. Kawahara. 2016. Low-cost soil moisture profile probe using thin-film capacitors and a capacitive touch sensor. *Sensors* 16(8): 1292.

Kramarenko, V. V., A.N. Nikitenkov, I.A. Matveenko, V.Y. Molokov and Y.S. Vasilenko. 2016. Determination of water content in clay and organic soil using microwave oven. *IOP Conference Series: Earth and Environmental Science* 43(1). https://doi.org/10.1088/1755-1315/43/1/012029.

Kramp, T., R. van Kranenburg and S. Lange. 2013. Introduction to the Internet of Things. In *Enabling Things to Talk*, 1–10. Springer, Berlin, Heidelberg.

Kulshreshtha, S. and C. Grant. 2003. Economic impact assessment of irrigation development and related activities in Manitoba. *Canadian Water Resources Journal* 28(1): 53–67. https://doi.org/10.4296/cwrj2801053.

Lehmann, P., S. Assouline and D. Or. 2008. Characteristic lengths affecting evaporative drying of porous media. *Physical Review E - Statistical, Nonlinear, and Soft Matter Physics* 77(5): 1–

16. https://doi.org/10.1103/PhysRevE.77.056309.

Leib, B.G., M. Hattendorf, T. Elliott and G. Matthews. 2002. Adoption and adaptation of scientific irrigation scheduling: Trends from Washington, USA as of 1998. *Agricultural Water Management* 55(2): 105–120.

Leib, B.G., J.D. Jabro and G.R. Matthews. 2003. Field evaluation and performance comparison of soil moisture sensors. *Soil Science* 168(6): 396–408.

Li, F. and D.M. Lawrence. 2017. Role of fire in the global land water budget during the twentieth century due to changing ecosystems. *Journal of Climate* 30(6): 1893–1908.

Li, J., D.W. Smith and S.G. Fityus. 2003. The effect of a gap between the access tube and the soil during neutron probe measurements. *Australian Journal of Soil Research* 41(1): 151–164. https://doi.org/10.1071/SR02054.

Ling, S.J., W. Moebs and J. Sanny. 2016. 8.1 Capacitors and Capacitance. *University Physics Volume 2*.

Magliulo, V., R. D'Andria and G. Rana. 2003. Use of the modified atmometer to estimate reference evapotranspiration in Mediterranean environments. *Agricultural Water Management* 63(1): 1–14. https://doi.org/10.1016/S0378-3774(03)00098-2.

Mahbub, M. 2020. A smart farming concept based on smart embedded electronics, internet of things and wireless sensor network. *Internet of Things* 9: 100161. https://doi.org/10.1016/j.iot.2020.100161.

Marazky, M.S.A., F.S. Mohammad and H.M. Al-Ghobari. 2011. Evaluation of soil moisture sensors under intelligent irrigation systems for economical crops in arid regions. *American Journal of Agricultural and Biological Sciences* 6(2): 287–300.

Masinda, M.M., F. Li, L. Qi, L. Sun and T. Hu. 2022. Forest fire risk estimation in a typical temperate forest in Northeastern China using the Canadian forest fire weather index: case study in autumn 2019 and 2020. *Natural Hazards* 111(1): 1085–1101.

Mason, P.E. 2011. Molecular dynamics study on the microscopic details of the evaporation of water. *Journal of Physical Chemistry A* 115(23): 6054–6058. https://doi.org/10.1021/jp1104517

Matula, S., K. Báťková and W.L. Legese. 2016. *Laboratory Performance of Five Selected Soil Moisture Sensors Applying Factory and Own Calibration Equations for Two Soil Media of Different Bulk Density and Salinity Levels*. *Sensors* 11, 2016. https://doi.org/10.3390/s16111912.

Moazenzadeh, R., B. Mohammadi, M.J.S. Safari and K. wing Chau. 2022. Soil moisture estimation using novel bio-inspired soft computing approaches. *Http://Www.Tandfonline.Com/Action/AuthorSubmission?JournalCode=tcfm20&page=instructions* 16(1): 826–840. https://doi.org/10.1080/19942060.2022.2037467

Nagahage, E.A.A.D., I.S.P. Nagahage and T. Fujino. 2019. Calibration and validation of a low-cost capacitive moisture sensor to integrate the automated soil moisture monitoring system. *Agriculture (Switzerland)* 9(7). https://doi.org/10.3390/agriculture9070141.

Nagata, Y., K. Usui and M. Bonn. 2015. Molecular Mechanism of Water Evaporation. *Physical Review Letters* 115(23): 1–5. https://doi.org/10.1103/PhysRevLett.115.236102.

Okasha, A.M., H.G. Ibrahim, A.H. Elmetwalli, K.M. Khedher, Z.M. Yaseen and S. Elsayed. 2021. Designing low-cost capacitive-based soil moisture sensor and smart monitoring unit operated by solar cells for greenhouse irrigation management. *Sensors* 21(16). https://doi.org/10.3390/s21165387.

Özgür, E. and K. Koçak. 2015. The effects of the atmospheric pressure on evaporation. *Acta*

Geobalcanica 1(1): 17–24. https://doi.org/10.18509/agb.2015.02.

Palaparthy, V.S., M.S. Baghini and D.N. Singh. 2013. Review of polymer-based sensors for agriculture-related applications. *Emerging Materials Research* 2(4): 166–180.

Pereira, L.S. and I. Alves. 2013. Crop water requirements, reference module in earth systems and environmental sciences Elsevier. https://doi. org/10.1016/B978-0-12-409548-9.05129-0, 2013.

Prat, M. 2002. Recent advances in pore-scale models for drying of porous media. *Chemical Engineering Journal* 86(1–2): 153–164. https://doi.org/10.1016/S1385-8947(01)00283-2.

Qandil, A. and A.I.O. Zaid. 2015. Considerations in the design and manufacturing of a load cell for measuring dynamic compressive loads. In *2015 Power Generation System and Renewable Energy Technologies (PGSRET)*, 1–6. IEEE.

Rajaram, K. and R. Sundareswaran. 2020. IoT Based Crop-Field Monitoring and Precise Irrigation System Using Crop Water Requirement. In *International Conference on Computational Intelligence in Data Science*, 291–304. Springer.

Regan, C.M., J.D. Connor, R.R. Segaran, W.S. Meyer, B.A. Bryan and B. Ostendorf. 2017. Climate change and the economics of biomass energy feedstocks in semi-arid agricultural landscapes: A spatially explicit real options analysis. *Journal of Environmental Management* 192: 171–183.

Reyes-González, A., J. Kjaersgaard, T. Trooien, C. Hay and L. Ahiablame. 2017. Comparative Analysis of METRIC Model and Atmometer Methods for Estimating Actual Evapotranspiration. *International Journal of Agronomy* 2017: 1–16. https://doi.org/10.1155/2017/3632501.

Rose, K., S. Eldridge and L. Chapin. 2015. THE INTERNET OF THINGS: AN OVERVIEW.

Understanding the Issues and Challenges of a More Connected World. *The Internet Society* (October): 80. http://electronicdesign.com/communications/internet-things-needs-firewalls-too.

Rotstayn, L.D., M.L. Roderick and G.D. Farquhar. 2006. A simple pan-evaporation model for analysis of climate simulations: Evaluation over Australia. *Geophysical Research Letters* 33(17): 1–5. https://doi.org/10.1029/2006GL027114.

Rowlandson, T.L., A.A. Berg, P.R. Bullock, E.R.T. Ojo, H. McNairn, G. Wiseman and M.H. Cosh. 2013. Evaluation of several calibration procedures for a portable soil moisture sensor. *Journal of Hydrology* 498: 335–344. https://doi.org/10.1016/j.jhydrol.2013.05.021.

Roy, S.K., S. Misra and N.S. Raghuwanshi. 2019. SensPnP: Seamless integration of heterogeneous sensors with IoT devices. *IEEE Transactions on Consumer Electronics* 65(2): 205–214. https://doi.org/10.1109/TCE.2019.2903351.

Roy, S.K., S. Misra, N.S. Raghuwanshi and S.K. Das. 2021. AgriSens: IoT-Based Dynamic Irrigation Scheduling System for Water Management of Irrigated Crops. *IEEE Internet of Things Journal* 8(6): 5023–5030. https://doi.org/10.1109/JIOT.2020.3036126.

Sakai, M., S.B. Jones and M. Tuller. 2011. Numerical evaluation of subsurface soil water evaporation derived from sensible heat balance. *Water Resources Research* 47(2): 1–17. https://doi.org/10.1029/2010WR009866.

Salvucci, G.D. 1997. Soil and moisture independent estimation of stage-two evaporation from potential evaporation and albedo or surface temperature. *Water Resources Research* 33(1): 111–122.

Sanchez-Lorenzo, A., S.M. Vicente-Serrano, M. Wild, J. Calbó, C. Azorin-Molina and J. Peñuelas. 2014. *Evaporation trends in Spain: A comparison of class A pan and Piché atmometer* *measurements*. *Climate Research* 3, pp. 269–280, 2014. https://doi.org/10.3354/cr01255.

Sayre, K.D. and P.R. Hobbs. 2004. The raised bed system of cultivation for irrigated production conditions. In *Sustainable Agriculture and the International Rice-Wheat System*, 354–372. CRC Press.

Schultz, P. 1991. On the falling-rate period. *Chemical Engineering & Technology: Industrial Chemistry-Plant Equipment-Process Engineering-Biotechnology* 14(4): 234–239.

Schulz, S., S. Darehshouri, E. Hassanzadeh, M. Tajrishy and C. Schüth. 2020. Climate change or irrigated agriculture–what drives the water level decline of Lake Urmia. *Scientific Reports* 10(1): 1–10.

Scott Lynn, N., C.S. Henry and D.S. Dandy. 2009. Evaporation from microreservoirs. *Lab on a Chip* 9(12): 1780–1788. https://doi.org/10.1039/b900556k.

Seethalakshmi, E., M. Shunmugam, R. Pavaiyarkarasi and S. Joseph. 2021. An automated irrigation system for optimized greenhouse using IoT. *Materials Today: Proceedings*.

Sharma, V. 2018. *Methods and Techniques for Soil Moisture Monitoring*. University of Wyoming Extension.

Shokri, N., P. Lehmann and D. Or. 2009. Characteristics of evaporation from partially wettable porous media. *Water Resources Research* 45(2).

Siddique, K.H.M., C. Johansen, N.C. Turner, M.-H. Jeuffroy, A. Hashem, D. Sakar, Y. Gan and S.S. Alghamdi. 2012. Innovations in agronomy for food legumes. A review. *Agronomy for Sustainable Development* 32(1): 45–64.

Singh, A.K., A.K. Bhardwaj, C.L. Verma, V.K. Mishra, A.K. Singh, S. Arora, N. Sharma and R.P. Ojha. 2019. Soil moisture sensing techniques for scheduling irrigation. *J. Soil Salin. Water Qual* 11: 68–76.

Singh, S.P. 2005. The role of technology in the emergence of the information society in India. *The Electronic Library*.

Smith, M., R. Allen and L. Pereira. 1998. Revised FAO methodology for crop-water requirements. *International Atomic Energy Agency (IAEA)* 51–58.

Srbinovska, M., C. Gavrovski, V. Dimcev, A. Krkoleva and V. Borozan. 2015. Environmental parameters monitoring in precision agriculture using wireless sensor networks. *Journal of Cleaner Production* 88: 297–307. https://doi.org/https://doi.org/10.1016/j.jclepro.2014.04.036.

Sreedeep, S., A.C. Reshma and D.N. Singh. 2004. Measuring soil electrical resistivity using a resistivity box and a resistivity probe. *Geotechnical Testing Journal* 27(4): 411–415.

Sri Ranjan, R. 2012. Plant-Controlled Atmometer for Measuring Crop Evapotranspiration. http://www.patentsencyclopedia.com/app/20100212409.

Stevens, J.B. 2007. Adoption of irrigatio scheduling methods in South AfricaUniversity of Pretoria, 2007.

Stirzaker, R.J., T.C. Maeko, J.G. Annandale, J.M. Steyn, G.T. Adhanom and T. Mpuisang. 2017. Scheduling irrigation from wetting front depth. *Agricultural Water Management* 179: 306–313.

Straatmann, Z., G. Stevens, E. Vories, P. Guinan, J. Travlos and M. Rhine. 2018. Measuring short-crop reference evapotranspiration in a humid region using electronic atmometers. *Agricultural Water Management* 195: 180–186. https://doi.org/10.1016/j.agwat.2017.10.007.

Surya, S.G., S. Yuvaraja, E. Varrla, M.S. Baghini, V.S. Palaparthy and K.N. Salama. 2020. An in-field integrated capacitive sensor for rapid detection and quantification of soil moisture. *Sensors and Actuators, B: Chemical* 321. https://doi.org/10.1016/j.snb.2020.128542.

Susha Lekshmi, S.U., D.N. Singh and M. Shojaei Baghini. 2014. A critical review of soil moisture measurement. *Measurement: Journal of the International Measurement Confederation* 54: 92–105. https://doi.org/10.1016/j.measurement.2014.04.007.

Vani, P.D. and K.R. Rao. 2016. Measurement and monitoring of soil moisture using cloud IoT and android system. *Indian Journal of Science and Technology* 9(31): 1–8.

Vani, P.D. and K.R. Rao. 2019. Implementation of Smart Agriculture using CloudIoT and its Geotagging on Android Platform. *International Journal of Engineering and Manufacturing* 9(2): 43–53. https://doi.org/10.5815/ijem.2019.02.04.

Varilly, P. and D. Chandler. 2013. Water evaporation: A transition path sampling study. *Journal of Physical Chemistry B* 117(5): 1419–1428. https://doi.org/10.1021/jp310070y

Vereecken, H., J.A. Huisman, H. Bogena, J. Vanderborght, J.A. Vrugt and J.W. Hopmans. 2008. On the value of soil moisture measurements in vadose zone hydrology: A review. *Water Resources Research* 44(4).

Vermesan, O. and P. Friess. 2013. *Internet of Things: Converging Technologies for Smart Environments and Integrated Ecosystems*. River publishers.

Villaroman, C.J., A. Espino, J. Lavarias and V. Taylan. 2018. Atmometer - Based irrigation scheduling system for drip - Irrigated onion (Allium cepa L.). *MATEC Web of Conferences* 192: 1–4. https://doi.org/10.1051/matecconf/201819203039.

Yamanaka, T. and T. Yonetani. 1999. Dynamics of the evaporation zone in dry sandy soils. *Journal of Hydrology* 217(1–2): 135–148.